MR Imaging in Hypertrophic Cardiomyopathy: From Magnet to Bedside[1]

Jan Bogaert, MD
Iacopo Olivotto, MD

Online SA-CME
See www.rsna.org/education/search/ry

Learning Objectives:

After reading the article and taking the test, the reader will be able to:

- Describe the phenotypic spectrum of abnormalities of hypertrophic cardiomyopathy (HCM)
- Discuss the need for risk profiling in HCM patients and family members
- Explain the interaction between phenotypic expression, functional and hemodynamic consequences, and potential adverse events
- Discuss the emerging role of MR imaging in screening, diagnosis, and risk profiling of HCM patients and family members
- Explain the potential value and the hurdles to be overcome for novel MR imaging techniques for risk profiling, such as late gadolinium enhancement MR imaging and T1 mapping

Accreditation and Designation Statement

The RSNA is accredited by the Accreditation Council for Continuing Medical Education (ACCME) to provide continuing medical education for physicians. The RSNA designates this journal-based activity for a maximum of 1.0 *AMA PRA Category 1 Credit*™. Physicans should claim only the credit commensurate with the extent of their participation in the activity.

Disclosure Statement

The ACCME requires that the RSNA, as an accredited provider of CME, obtain signed disclosure statements from the authors, editors, and reviewers for this activity. For this journal-based CME activity, author disclosures are listed at the end of this article.

[1] From the Department of Radiology, Gasthuisberg University Hospitals Leuven, Herestraat 49, B-3000 Leuven, Belgium (J.B.); and Referral Center for Myocardial Diseases, Azienda Universitaria Careggi, Florence, Italy (I.O.). Received July 23, 2013; revision requested September 18; revision received October 21; accepted November 14; final version accepted December 13; final review by authors May 20, 2014. **Address correspondence to** J.B. (e-mail: *jan.bogaert@uz.kuleuven.ac.be*).

Hypertrophic cardiomyopathy (HCM), the most common genetically transmitted cardiac disorder, has been the focus of extensive research over the past 50 years. HCM is a multifaceted disease with highly heterogeneous genetic background, phenotypic expression, clinical presentation, and long-term outcome. Though most patients have an indolent course with a life expectancy comparable to that of the general population, early diagnosis and accurate risk profiling are essential to identify the sizeable subset at increased risk of sudden cardiac death or disease progression and heart failure–related complications, requiring aggressive management options. Imaging has a central role in the diagnosis and prognostic assessment of HCM patients, as well as screening of potentially affected family members. In this context, magnetic resonance (MR) imaging has recently emerged as an ideal complement to transthoracic echocardiography. Its multiparametric approach, fusing spatial, contrast, and temporal resolution, provides the clinician with detailed characterization of the HCM phenotype and assessment of its functional consequences including causes and site of dynamic obstruction, presence and extent of myocardial perfusion abnormalities, and fibrosis. Moreover, MR is key in differentiating HCM from "phenocopies"—that is, hearts with similar morphology but profoundly different etiology, such as amyloid or Anderson-Fabry disease. Long term, the incremental information provided by MR is relevant to planning of septal reduction therapies, identification of the early stages of end-stage progression, and stratification of arrhythmic risk. The aim of this review is to depict the increasingly important role of MR imaging in relation to the complexity of HCM, highlighting its role in clinical decision making.

Online supplemental material is available for this article.

Hypertrophic cardiomyopathy (HCM), the most common inherited cardiomyopathy, represents one of the most fascinating diseases in cardiovascular medicine, attracting the interest of physicians, geneticists, and scientists worldwide. This disorder is characterized by inappropriate myocardial hypertrophy occurring in the absence of any detectable cardiac or systemic cause, such as aortic stenosis arterial hypertension (1). The diagnosis requires exclusion of disease entities that may lead to inappropriate myocardial wall thickening of other etiologies, such as infiltrative and metabolic storage diseases (the so-called phenocopies). Familial transmission is found in about 60% of probands and generally follows an autosomal-dominant pattern (2). In most patients, HCM is caused by mutations in one of the genes encoding cardiac sarcomere proteins (3); however, many other genes have been shown to cause rare forms of HCM, including Z-disk proteins and mitochondrial genes. Of note, disease-causing mutations do not account for the great variability of phenotypes and clinical profiles observed even within the same families, pointing to additional and poorly understood genetic, epigenetic, and environmental factors as critical modifiers of HCM expression (4). Adding to this complexity is the observation that mutations in the same sarcomere protein genes may result in dilated, restrictive, and noncompaction phenotypes rather than HCM.

As shown in population-based studies, most HCM patients seem to remain asymptomatic and undiagnosed in the community and have normal life expectancy. Not infrequently, however, the presence of HCM may be detected on an electrocardiogram or at echocardiography during pre-participation athletic screening or routine medical check-ups. Conversely, symptomatic patients will actively seek medical attention due to palpitations, syncope, exertional dyspnea (with or without chest pain), systemic thromboembolism, and stroke (5). These symptoms are caused by the interplay of features such as intraventricular obstruction, microvascular ischemia, diastolic heart failure, sustained supraventricular arrhythmias, and recurrent nonsustained ventricular arrhythmias. Rarely, HCM may present with cardiac arrest and sudden cardiac death (SCD). To date, HCM represents the most commonly identified cause of premature SCD due to malignant ventricular arrhythmias in young individuals and athletes (2,5).

Essentials

- Any attempt toward a simple definition of hypertrophic cardiomyopathy (HCM) has been hampered by the fact that, rather than a single well-defined entity, the disease includes a spectrum of conditions; clinical presentation ranges from asymptomatic individuals with mild phenotypes—or even phenotype-negative mutation carriers—to severely symptomatic patients with dynamic left ventricular outflow obstruction or hypokinetic-restrictive end-stage disease.
- Disease-causing sarcomere gene mutations do not account for the great variability of HCM phenotypes and clinical profiles—observed even within the same families—pointing to additional and poorly understood genetic, epigenetic, and environmental factors as critical modifiers of its ultimate expression; adding to this complexity, mutations in the same cardiac sarcomere protein genes may result in dilated, restrictive, and noncompaction phenotypes rather than HCM.
- Since its introduction in the mid-1980s, cardiac MR imaging has evolved into a multiparametric imaging modality allowing a truly comprehensive patient- and disease-tailored appraisal of HCM, providing information on major areas of interest including cardiac phenotype, its functional and hemodynamic characterization, presence and extent of microvascular dysfunction, and myocardial fibrosis.

Historical Perspective: How Imaging Has Changed Our Perception of the Disease

Though several reports suggest that HCM had already been recognized centuries ago, it was not until the late 1950s that the disease was brought to the attention of the international medical community (6). Brock, Morrow et al, and Braunwald et al reported functional obstruction of the left ventricle (LV) occurring at the LV outflow tract, simulating aortic stenosis, an entity defined as "idiopathic hypertrophic subaortic stenosis" (7–9). Nearly at the same time, Teare (10) reported asymmetric hypertrophy of the heart involving the interventricular septum and anterior LV wall in young adults who died suddenly, half of whom were asymptomatic prior to their death. Interestingly, the pathologic picture was virtually the same in all these individuals, one of bizarre and disorganized arrangement of muscle bundles (the so-called myocardial disarray) with hypertrophy of individual muscle fibers and their nuclei (Fig 1). Not infrequently, extensive replacement fibrosis was found, mainly at the center of the hypertrophied myocardium, deemed to be postischemic in origin. At the same time, the genetic nature of HCM was suspected, based on the autosomal dominant inheritance pattern in the family of one of the victims (11).

Historically, any attempt toward the ultimate definition of HCM has been hampered by the fact that, rather

Published online
10.1148/radiol.14131626 **Content codes:** CA MR

Radiology 2014; 273:329–348

Abbreviations:
HCM = hypertrophic cardiomyopathy
LGE = late gadolinium enhancement
LV = left ventricle
SCD = sudden cardiac death
SSFP = steady-state free precession
3D = three-dimensional

Conflicts of interest are listed at the end of this article.

Figure 1

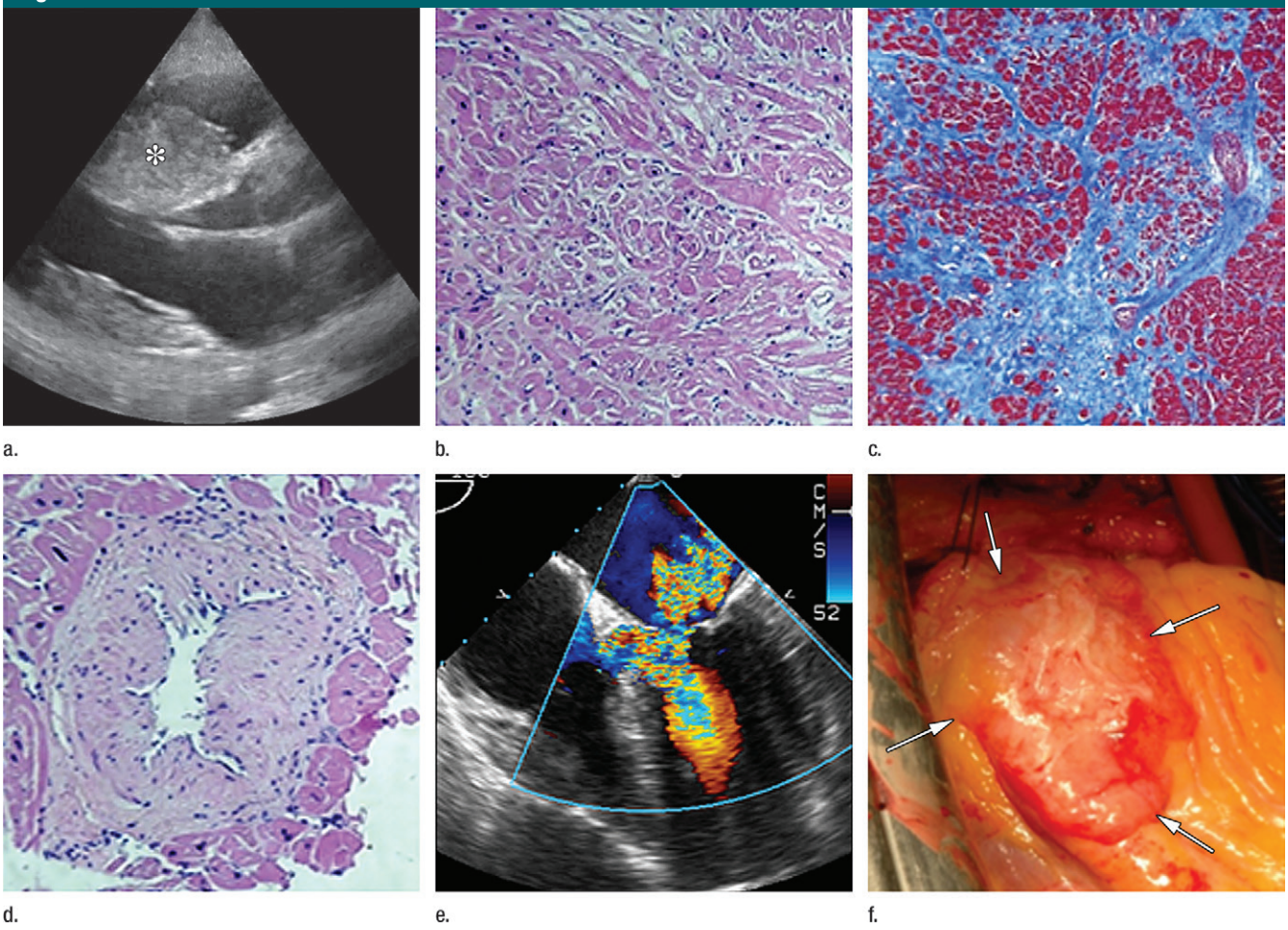

Figure 1: Phenotypic heterogeneity of HCM beyond LV hypertrophy. **(a)** Transthoracic echocardiogram (parasternal long-axis view) shows important thickening of the basal and mid-part of the interventricular septum (*). At histologic examination, **(b)** myocardial disarray (hematoxylin-eosin; magnification, ×10), **(c)** myocardial replacement fibrosis (trichromic stain; magnification, ×10), and **(d)** severe remodeling of the intramural arterioles (hematoxylin-eosin; magnification, ×10) prevail. **(e)** At transesophageal echocardiography, LV outflow tract obstruction with secondary mitral regurgitation is often present in HCM patients. **(f)** Midventricular HCM may cause the formation of an apical LV aneurysm (arrows).

than a single well-defined entity, the disease seemed to include a spectrum of conditions. This led to an impressive proliferation in disease nomenclature (4), many of which were based on the concept of "stenosis" or "obstruction." The term *hypertrophic cardiomyopathy* ultimately gained universal consensus, following recognition that only a subset of patients have an obstructive form of the disease. Genotype-positive, phenotype-negative individuals, however, belong to the spectrum of HCM despite the absence of hypertrophy, raising further potential controversy over the issue of "nonhypertrophic" HCM.

The pioneering studies from the 1960s marked the beginning of extensive clinical, pathologic, genetic, and molecular research into this highly complex disease. Owing to these efforts, our perception of HCM has gradually shifted from that of a rare and malignant disease to the current perspective of a relatively common and often favorable condition, compatible with normal life expectancy (4). This paradigm shift is largely due to improved knowledge of the natural evolution of HCM in unselected, community-based patient populations, as compared with the highly selected early cohorts seen at international tertiary referral centers (4,5). Because an unfavorable outcome is relatively uncommon in HCM populations, early recognition and risk stratification are both challenging and crucial in identifying those patients who may benefit from aggressive management, while allowing cautious reassurance in the remainder (5).

At the time of the earliest HCM investigations, the only means of assessing pathophysiology in vivo was LV catheterization. In the absence of direct visualization of the LV and mitral apparatus, hemodynamic studies allowed the identification of subaortic gradients but

Figure 2

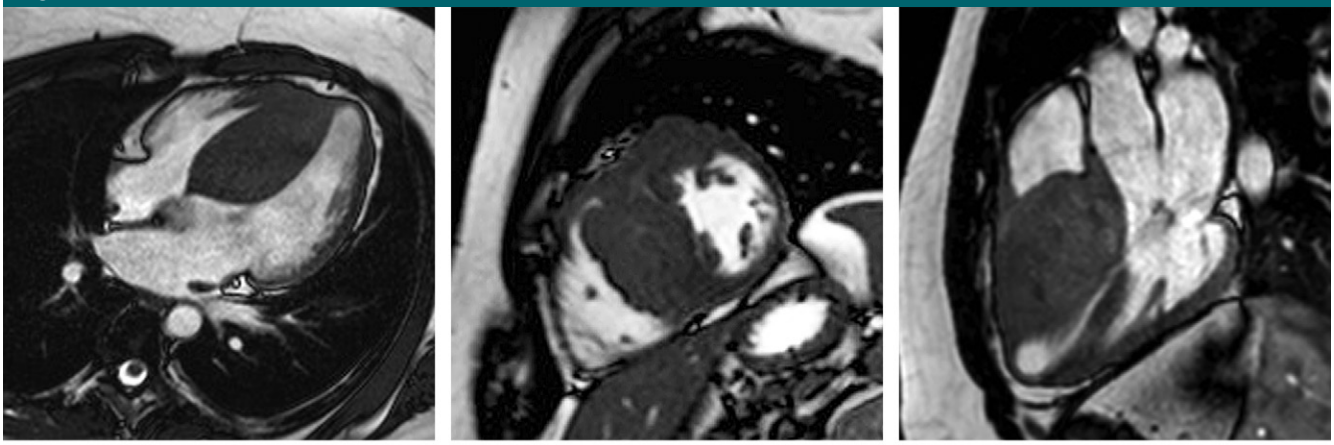

a. b. c.

Figure 2: Severe form of asymmetric septal HCM in 20-year-old man. Steady-state free precession (SSFP) images (repetition time msec/echo time msec, 2.7/1.4; 55° flip angle; 1.4 × 2.0-mm in-plane resolution) are shown **(a)** in horizontal long-axis, **(b)** in midventricular short-axis, and **(c)** along the LV outflow tract. The location and extent of hypertrophy as well as the effect of the hypertrophied myocardium on the LV outflow tract can be well appreciated by using cine imaging in several imaging planes. The maximal thickness of the ventricular septum is 43 mm. Note the extension of hypertrophy toward the right ventricular apex and free wall.

not of their cause, which remained an enigma until the advent of echocardiography in the late 1960s. Echocardiography has proven critical in developing a comprehensive understanding of HCM, by allowing recognition of its true prevalence, phenotypic heterogeneity, and pathophysiologic implications. The description of systolic anterior motion of the mitral leaflets finally unraveled the mystery of LV outflow tract obstruction that had lasted over a decade (12,13). It also explained the impressive results of surgical myectomy—an operation introduced as a leap of faith, well before the cause of obstruction was discovered (14). Subsequently, echocardiography demonstrated that most HCM patients develop outflow obstruction either in resting conditions or with exercise (15,16) and revealed a spectrum of HCM manifestations beyond LV hypertrophy, ranging from mitral valve abnormalities to apical aneurysms (17,18). From an epidemiologic perspective, echocardiography has led to an accurate estimate of HCM prevalence in the general population (around 1:500) and appropriate screening of HCM family members (19). In the clinical setting, transthoracic echocardiography represents the reference standard for serial evaluation of time-related changes in clinical and hemodynamic status, identification of HCM-related complications, and assessment of pharmacologic and invasive treatment options.

Several noninvasive imaging modalities have been utilized in HCM aside from echocardiography. Thallium-201 single-photon emission computed tomography (SPECT) and positron emission tomography (PET) have been key in demonstrating myocardial perfusion defects and blunted coronary reserve, subtended by marked anatomic remodeling of the coronary microcirculation (20–22). Computed tomography (CT), currently performed with multidetector technology, is particularly helpful in visualizing subtle morphologic abnormalities of the HCM phenotype, such as myocardial crypts and coronary artery abnormalities including myocardial bridging, anomalous origin, or superimposed atherosclerotic disease (23,24). Last but not least, since its introduction in the mid-1980s, cardiac magnetic resonance (MR) imaging has now evolved into a multiparametric imaging modality allowing a truly comprehensive patient- and disease-tailored appraisal of HCM, providing information on major areas of interest including cardiac phenotype, its functional and hemodynamic characterization, presence and extent of microvascular dysfunction, and myocardial fibrosis (Fig 2) (25).

Characterization of Phenotype and Diagnosis

Clinical Aspects

The "classic" HCM phenotype is that of a hypertrophied, nondilated LV (Figs 1, 2). LV hypertrophy typically arises during adolescence and is usually complete by young adulthood, though onset of phenotype may occur at virtually any age, including in utero and older than 60 years (26). When investigating a patient with a potential diagnosis of HCM, however, it is important to consider that the phenotypic spectrum expands well beyond the mere presence of LV hypertrophy, to include an array of morphofunctional manifestations such as abnormalities of papillary muscles and mitral apparatus, deep myocardial crypts, myocardial bridging of coronary arteries, left atrial remodeling, areas of LV noncompaction, apical aneurysms, LV outflow obstruction, microvascular dysfunction, and myocardial fibrosis (Tables 1, 2). Furthermore, in 5%–15% of patients adverse LV remodeling occurs with progressive dilation, wall thinning, dysfunction, and

Table 1

The Different Manifestations and Outcomes of HCM: From Genotype-Positive/Phenotype-Negative to Refractory Heart Failure

				LGE*			
Phenotype	Prevalence	Phenotypic Expression	LV Ejection Fraction	Prevalence	Percentage of LV Mass	Location	Risk of SCD
Nonhypertrophic phase		Myocardial wall thickness: normal/borderline increase Deep myocardial crypts Accessory apical-basal muscle bundle Abnormal mitral valve/papillary muscles Microvascular dysfunction: ? Interstitial myocardial fibrosis: ?	Normal	Rare/absent	Limited	Midwall	Exceptional
"Classic" phenotype	75%	Myocardial hypertrophy: overt LV obstruction (70%) Left atrium dilatation: mild to moderate, severe when LV outflow tract obstruction present Microvascular dysfunction Myocardial bridging	Increased (> 65%)	Common (± 40%)	2% (Median)	Midwall	Low (0.5%–1%/year)
Adverse remodeling	15%	Myocardial hypertrophy: evident but progressive thinning may occur LV obstruction: less common, loss of prior obstruction Left atrium dilatation: moderate/severe Microvascular dysfunction: moderate to severe Apical aneurysm	50%–65%	Common (> 50%)	10%–15%	Midwall/transmural	Probably intermediate
"End-stage" HCM	±5%	"Dilated – hypokinetic" form: LV obstruction: absent Frequent LV wall thinning Severe microvascular dysfunction May mimic dilated cardiomyopathy "Restrictive – hypokinetic" form: Small LV Severe biatrial dilatation May mimic restrictive cardiomyopathy	<50%	Common (75%–100%)	>25%	Midwall/transmural "infarct"-like	High (10%/year)

* LGE = late gadolinium enhancement.

Table 2

From Pathophysiology to Clinical Decision Making in HCM: Insights from MR Imaging

Anatomic Substrates	Morphofunctional Correlates	Clinical End Points	Relevant Indications
Myocardial hypertrophy*	Atrial dilatation*	Atrial fibrillation	Anticoagulation
Myofiber disarray	Adverse LV remodeling*	Stroke-thrombo-embolic events	Ablation of atrial fibrillation
Replacement fibrosis*	LV outflow tract /midventricular obstruction*	SCD	Implantable cardioverter defibrillator implantation
Microvascular remodeling	Mitral regurgitation*	Heart failure	Surgical myectomy/alcohol ablation
Interstitial fibrosis†	Diastolic dysfunction†	"End-stage" HCM	Antiremodeling pharmacological therapy
Mitral (sub)valvar abnormalities*	Microvascular hypoperfusion†		Heart transplant
Myocardial crypts*	Apical aneurysm*		
Accessory apical-basal muscle bundle*	Arrhythmogenesis		
Myocardial bridging†			
Noncompaction*			

* Routinely assessed at MR imaging.

† Potential role of MR imaging.

Figure 3

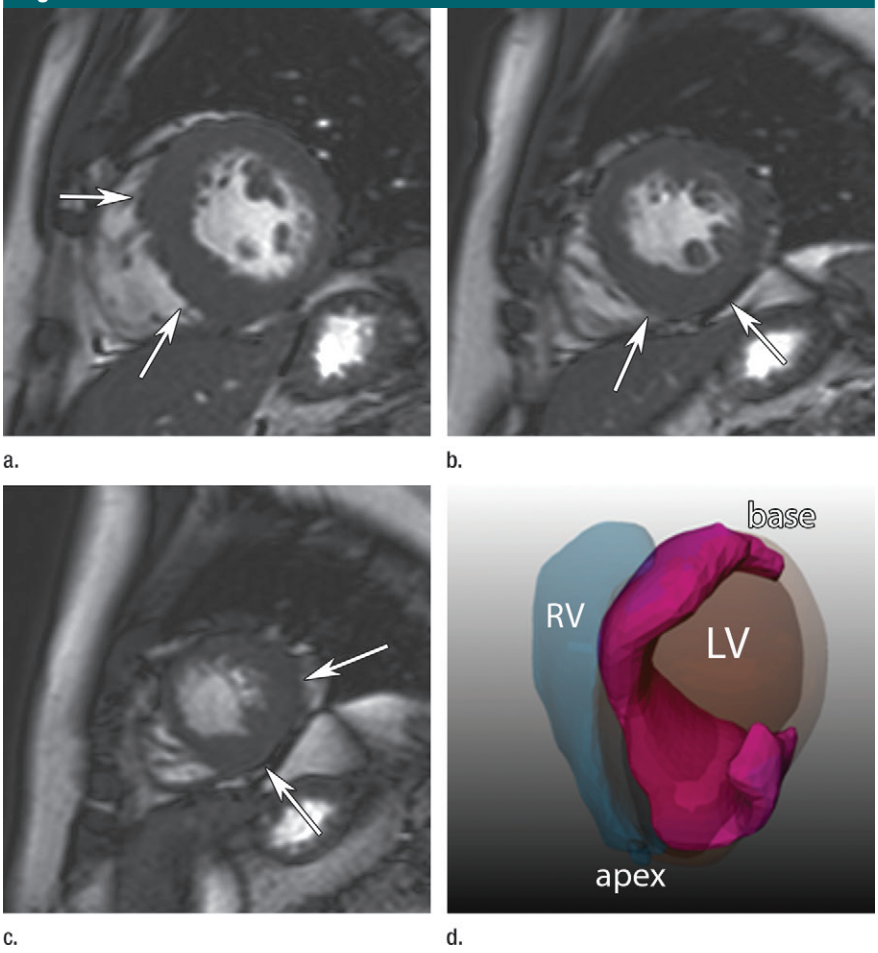

Figure 3: Three-dimensional spread of hypertrophy following a counter clockwise spiral in a 38-year-old man with asymmetric septal HCM. **(a–c)** Short-axis SSFP images (2.7/1.4, 55° flip angle, 1.4 × 2.0-mm in-plane resolution) at end-diastole at three levels from LV base (**a**) to apex (**c**) allow one to appreciate the spiral nature of the hypertrophied myocardium (arrows). **(d)** Volume-rendered 3D image of the heart (anterior view). The hypertrophied myocardium is in red. (Reprinted, with permission, from reference 34.) See Movie 1 (online).

evolution toward overt heart failure, a phenomenon called "end-stage" HCM, resembling dilated or, more frequently, restrictive cardiomyopathy (Table 1) (27–29).

Each of these elements should be carefully sought and considered to establish a diagnosis and characterize the severity of HCM disease expression (Table 2).

In probands, HCM is considered present when maximum LV wall thickness is 15 mm or greater (or the equivalent relative to the body surface area in children) (30). In a minority of patients, the increase in wall thickness can be extreme, exceeding 30 mm (Fig 2). Borderline increases in wall thickness (ie, 12–14 mm) may be difficult to interpret, although a positive family history of HCM suggests this diagnosis in this gray zone (4). Most often, the distribution of hypertrophy is asymmetric and segmental, while diffuse, concentric forms of HCM represent a minority (about 5%) (4,30). Notably, in about 20% of HCM patients LV mass index values are normal at MR imaging (31). In 70% of patients the hypertrophied regions involve the basal segments of the anterior ventricular septum and anterior wall (32). Other less frequent locations are the mid- and lower portion of the ventricular septum often extending to the inferior wall, the anterolateral wall, and the apex. Hypertrophy of the papillary muscles and right ventricle often concurs (33). Exploiting the three-dimensional (3D) features of cine MR imaging, it was shown that in most HCM patients the hypertrophied myocardium follows a longitudinal pattern along a spiral trajectory in a counter clockwise direction from the base to the apex of the LV (Fig 3, Movie 1 [online]) (34). The magnitude of spiraling ranged from minimal—following an almost straight trajectory—to marked, covering nearly the entire circumference of the LV.

Apical HCM accounts for less than 10% of HCM patients, although it is more prevalent in Japanese cohorts, typically associated with giant inverted anterolateral T-waves on the electrocardiogram (Fig 4, Movie 2 [online]) (35). Furthermore, apical extension of LV hypertrophy can be found in 10% of patients with classic septal HCM, suggesting that both phenotypic expressions may coexist (34). Traditionally, the same cutoff value (≥15 mm) is used to diagnose apical HCM (35), although a lower cutoff is probably advisable, given that the myocardium is normally thinner at this level (36). Apical HCM is generally not associated with outflow obstruction and is clinically well tolerated. However, when severe, it can determine extensive cavity obliteration and restrictive pathophysiology, causing severe congestive symptoms. Severe midapical forms of HCM can cause dynamic obstruction at the midventricular level. Occasionally, these patients develop a noncontractile apical aneurysm (present in about 2% of consecutive HCM patients) which portends increased arrhythmic and cardioembolic risk (Table 2) (37).

Abnormalities in morphology and function of the mitral valve apparatus are often seen in HCM patients (38), the most striking being a marked elongation of both mitral leaflets. These abnormalities may also be present in genotype-positive family members with none of the other phenotypic expressions of HCM (Table 1). Mitral leaflet elongation

Figure 4

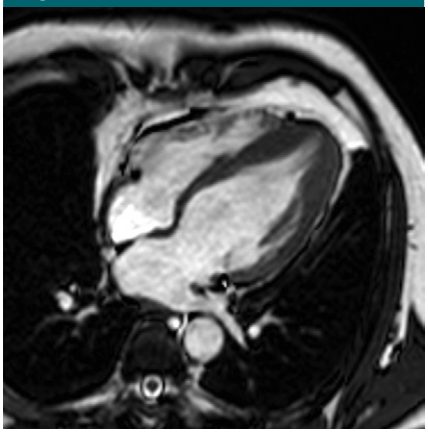

Figure 4: Apical HCM in a 54-year-old man. Cine SSFP MR image (2.7/1.4, 55° flip angle, 1.4 × 2.0-mm in-plane resolution) in horizontal long-axis plane at end-diastole is shown. The LV apex is clearly hypertrophied (maximal wall thickness, 18 mm). See Movie 2 (online).

Figure 5

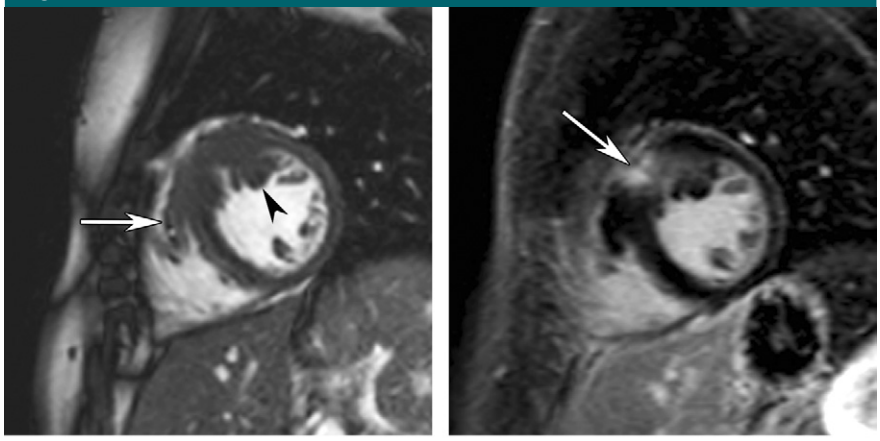

a. b.

Figure 5: Asymmetric septal HCM in a 24-year-old asymptomatic woman with septal hypertrophy at routine echocardiography and electrocardiography. On **(a)** midventricular short-axis cine SSFP MR image (2.7/1.4, 55° flip angle, 1.4 × 2.0-mm in-plane resolution) and **(b)** LGE MR image (4.3/1.3, 260-msec inversion time), the focal thickening of the anteroseptal LV wall can be well appreciated (maximal thickness, 19 mm). Note concomitant hypertrophy of the adjacent right ventricular trabeculations (arrow, **a**) and the anterior papillary muscle (arrowhead, **a**), which is medially displaced. Measurements of myocardial wall thickness should not include these paraseptal structures. Following contrast agent administration, subepicardial enhancement is present in the thickened LV wall (arrow, **b**).

is considered an important determinant of dynamic obstruction (Table 2). Subvalvular abnormalities include hypertrophy and variation of the papillary muscle in appearance (eg, bifid), number, and implantation (ie, short chordae or direct papillary muscle insertion into the mitral leaflets) (Fig 5). Anteroapical displacement of the anterolateral papillary muscle may contribute to the severity of LV outflow obstruction (39,40).

Deep muscular clefts or crypts (ie, narrow, blood-filled myocardial invaginations) usually located in the basal inferoseptal LV wall have been frequently reported in HCM patients (41). These are considered among its distinctive morphologic expressions, occurring both in patients and in genotype-positive family members (Table 2) (42,43). Likewise, regions of noncompaction (ie, excessive myocardial trabeculations), most typically at the inferior and lateral apical segments of the LV, are increasingly reported in HCM patients. While the identification of these areas bears doubtful (if any) clinical importance, noncompaction may represent a marker of genetic transmission in family members without hypertrophy (Table 2).

Finally, myocardial bridging of the left anterior descending coronary artery belongs to the phenotypic spectrum of HCM (Table 2). Early studies have reported an association between coronary bridging and risk of SCD, particularly in children. However, subsequent studies in larger cohorts have shown that bridging is in most instances a benign feature (24,44). Only when severe and extensive, myocardial bridging may be the cause of symptoms and ventricular arrhythmias in young HCM patients, whereas its clinical relevance appears questionable in adult patients with no or mild symptoms.

Role of MR Imaging in Morphofunctional Characterization of HCM

There is an emerging role for MR imaging in the evaluation of HCM phenotype and its differentiation from phenocopies (Table 3) (32,45,46). MR imaging is the most accurate technique to obtain correct measurements of maximal wall thickness in echocardiographically "difficult" regions of the LV, increasing the diagnostic yield by identifying subtle forms of myocardial hypertrophy (Fig 6) (47). Furthermore, MR may be helpful in risk stratification by identifying massive LV hypertrophy or extensive areas of myocardial fibrosis heralding disease progression (45). Though adequate assessment can be achieved by using black-blood fast T1-weighted spin-echo MR imaging, bright-blood balanced SSFP cine MR has the advantage of providing dynamic images with high spatial and contrast resolution, thereby fusing morphologic and functional assessment into one MR sequence (Fig 2). Dynamic cine imaging allows assessment of myocardial motion patterns, visualization of hemodynamic abnormalities (such as flow void due to acceleration and/or turbulence by LV outflow tract obstruction, midventricular gradients, or mitral regurgitation), and calculation of ventricular volumes and myocardial mass. Use of 3D bright-blood SSFP imaging using a respiratory navigator pulse provides high-spatial-resolution morphologic images of the coronary artery anatomy and papillary muscle abnormalities (46).

At present there are no guidelines identifying standardized MR imaging planes in HCM patients. To assess the

Table 3

Overview of Standard, Optional, and Research MR Sequences to Study HCM

MR Sequence	Purpose
Standard	
Scout views	Determination of cardiac image planes
SSFP cine imaging	LV/right ventricle volumes, ejection fraction, and mass
	Myocardial wall thickness
	Regional function (motion/thickening)
	Geometric pattern of hypertrophy
	Calculation of LV outflow tract diameter/area
	Mitral regurgitation (visual analysis)
	Myocardial crypts
	Left atrial size and function
LGE imaging	Myocardial replacement fibrosis
	Evaluation of effects of therapy (scar tissue)
	Thrombus formation in left atrial appendage (atrial fibrillation)
Velocity-encoded cine imaging	Hemodynamic consequences of obstruction (gradient calculation
	Quantification of mitral regurgitant volume/fraction
	Diastolic (dys)-function (mitral inflow/pulmonary vein flow)
Optional	
T1-weighted fast spin-echo imaging	Morphologic evaluation (if insufficient information with cine imaging)
3D SSFP imaging	Detailed anatomic information (eg, papillary muscle abnormalities/crypts)
T1 mapping	Quantification of extracellular volume reflecting myocardial interstitial fibrosis
T2-weighted imaging/T2 mapping	Myocardial edema (eg, acute ischemia)
Rest/stress perfusion imaging	Microvascular function
	Hemodynamic significant coronary artery stenoses
MR tagging	Myocardial deformation analysis (two-dimensional/3D)
3D contrast-enhanced MR angiography	Pulmonary vein anatomy (preablation vein imaging in atrial fibrillation patients)
Research	
Diffusion imaging	Myofiber disarray
MR spectroscopy	Metabolic spectra

Figure 6

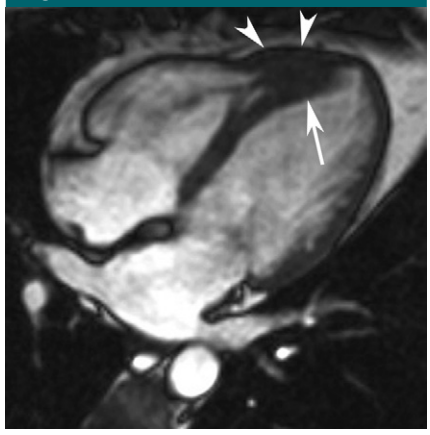

Figure 6: Focal HCM in a 47-year-old woman with family history of HCM. Horizontal long-axis cine SSFP MR image (2.7/1.4, 55° flip angle, 1.4 × 2.0-mm in-plane resolution) shows focal thickening of the apical part of the ventricular septum (arrow) extending to the adjacent RV free wall (arrowheads).

spatial extent of hypertrophy, we recommend the acquisition of a complete set of contiguous short-axis images and at least one vertical and one horizontal long-axis image. Important additional planes include those along the LV outflow tract (Fig 2). Apical HCM, sometimes difficult to assess with echocardiography because of near-field problems of the echo probe, is optimally visualized with MR. Even when mild, apical hypertrophy should be considered present when the normal morphologic thinning of the LV myocardial wall toward the apex is absent (Fig 4). When the acoustic window is suboptimal, the differential diagnosis between apical HCM and isolated LV noncompaction may be challenging with echocardiography, and MR imaging may be decisive in reaching the correct diagnosis.

When the HCM phenotype is fully expressed, echocardiography generally allows a reliable and unequivocal diagnosis. Occasionally, however, the differential diagnosis with phenocopies may be challenging. MR imaging has evolved into an excellent tool allowing further characterization of "thick-walled" ventricles (Table 4). In this case however, bright-blood cine MR imaging often does not suffice, necessitating a more comprehensive approach including LGE and velocity-encoded cine MR imaging (Table 3).

Differential Diagnosis

Physiologic remodeling resulting from regular and intensive exercise, generally known as "athlete's heart," may cause LV hypertrophy. However, LV wall thickness increase is uncommon (even in elite athletes), concentric, usually mild, and paralleled by a proportional increase in volume of both ventricles (Table 4) (48,49). End-diastolic wall thickness does not generally exceed 13 mm in male and 11 mm in female athletes. Thickness values greater than 15 mm should be considered definitely abnormal (50). In the "grey zone" of LV wall thickness (>12 mm to 15 mm), a correct diagnosis is as difficult as it is important, in that it may prevent disease-related complications in the presence of true HCM or allow continuation of a normal life, including competitive activities, when HCM can be excluded (51). Decision making in this gray area can never be based on a single piece of information, and it involves consideration of a number of additional elements such as the electrocardiography pattern, diastolic indexes, family history, genetic testing, and response to detraining. Of note, the effects of detraining on LV hypertrophy can be

accurately assessed by means of serial cine MR imaging.

Increased LV afterload due to systemic arterial hypertension or aortic stenosis may simulate HCM. Aortic stenosis is generally easy to rule out with echocardiography; in complex cases, however, the presence and hemodynamic consequences of aortic stenosis can be assessed with MR by a combination of cine imaging and velocity-encoded imaging, enabling accurate measurement of the aortic valve orifice and transvalvular pressure gradient (52). Differentiating HCM from hypertensive cardiomyopathy may be more challenging, particularly in hypertensive patients manifesting asymmetric LV hypertrophy. Of note, while the spectrum of geometric adaptations in hypertensive cardiomyopathy is complex, most untreated patients with systemic arterial hypertension have normal LV mass and wall thickness, while "typical" hypertensive concentric hypertrophy occurs only in a minority (53).

LV noncompaction belongs to the phenotypic spectrum of mutations in genes encoding proteins of the cardiac sarcomere (Table 2). Of note, the primary nature of isolated LV noncompaction as a distinct cardiomyopathy is currently being challenged as aspects of noncompaction can be observed in virtually all forms of genetic heart disease, as well as in congenital malformations (3,54) and athletes (55). MR is increasingly used to investigate patients with suspected LV noncompaction, although the lack of reliable MR criteria for diagnosis leads to a substantial risk of overestimating its prevalence (56,57) (Table 4). Isolated noncompaction may mimic apical HCM when particularly severe and occurring at the midapical LV level, where it may be hard to recognize by using echocardiography.

Cardiac amyloidosis is a rare but important phenocopy of HCM. Cardiac involvement may be the presenting feature or may be discovered while investigating a patient manifesting noncardiac features of the disease. Prognosis in these patients is driven by the cause of amyloidosis and by the severity of cardiac involvement (58). Diffuse amyloid deposition involves left and right ventricular myocardium in a concentric pattern and extends to the valve leaflets, atrial walls, and septum; mild concentric pericardial effusion may coexist. LV systolic function may be relatively spared (although often reduced), whereas severe diastolic dysfunction with restrictive pathophysiology is the rule in advanced disease. LGE imaging is extremely helpful in differentiating cardiac amyloidosis from HCM, by revealing characteristic patterns of myocardial enhancement, including global, subendocardial, less often patchy or diffuse LGE distribution within the LV (59). These patterns are determined by the distribution and severity of amyloid deposition and are related to outcome (Fig 7) (60,61). In cardiac amyloidosis, altered gadolinium kinetics in the blood and myocardium—that is, diffuse LGE associated with increased clearance of gadolinium from the blood pool, producing small differences in T1 relaxation time between blood and myocardium—causes the ventricular cavity to appear dark while the myocardium remains bright irrespective of the inversion time used. Thus, if the administration as well as the dosage of gadolinium-based contrast medium are correct, this pattern should immediately raise the suspicion of amyloid infiltration of the LV, particularly in the presence unexplained myocardial hypertrophy. Recently, non–contrast-enhanced T1 mapping and equilibrium contrast enhancement MR imaging have been proposed as appealing noninvasive techniques to diagnose and to quantify the amyloid burden of the heart, potentially predicting outcome (59,62).

Cardiomyopathies associated with metabolic storage diseases (eg, Anderson-Fabry, Pompe, Gaucher, and Neimann-Pick disease) represent rare, genetically determined phenocopies, characterized by a variety of cardiac signs and symptoms including LV hypertrophy, diastolic dysfunction, arrhythmias, microvascular ischemia, and heart failure. MR imaging may be useful at various stages in establishing the diagnosis and evaluating prognosis and disease progression, as well as in monitoring the effects of management, including enzyme-replacement therapy. About half of Anderson-Fabry patients show areas of LGE in the LV inferolateral wall reflecting focal scarring, which has been proposed as a substrate for arrhythmias and SCD (63). Intramyocardial glycosphingolipid accumulation may be measured with non–contrast-enhanced T1 mapping, showing a

Table 4

Differential Diagnosis in LV Hypertrophy

Morphologic Pattern	Differential Diagnosis	Useful Clues (Suggesting HCM)
Mild LV hypertrophy	Athlete's heart	Small/normal size LV Elongated mitral valve/SAM Myocardial crypts Accessory apical-basal muscle bundle Presence of LGE (rarely present)
Mild-moderate LV hypertrophy	Hypertensive heart disease Aortic stenosis	Normal aortic root Normal aortic valve Elongated mitral valve/SAM Extensive/patchy LGE
Severe LV hypertrophy	Amyloidosis Other storage diseases	Spared atrial walls and septum Lack of pericardial effusion Septal as opposed to endocardial LGE Elongated mitral valve/SAM Preserved systolic function
Apical LV hypertrophy	LV noncompaction	Thickened apical myocardium (as opposed to extensive trabeculations)

Note.—SAM = systolic anterior motion.

Figure 7

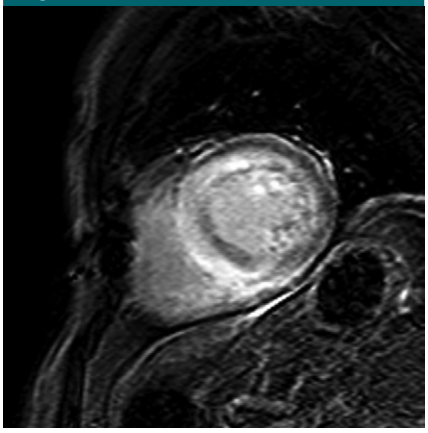

Figure 7: Cardiac amyloidosis in a 71-year-old woman with diastolic heart failure and nonsustained ventricular tachycardia at presentation. Midventricular short-axis LGE MR image (4.3/1.3, 270-msec inversion time) shows concentric LV hypertrophy with septal wall thickness (23 mm), decreased LV ejection fraction (38%), and increased LV mass (262 g). Marked, inhomogeneous enhancement is seen in both ventricles following contrast agent administration.

Figure 8

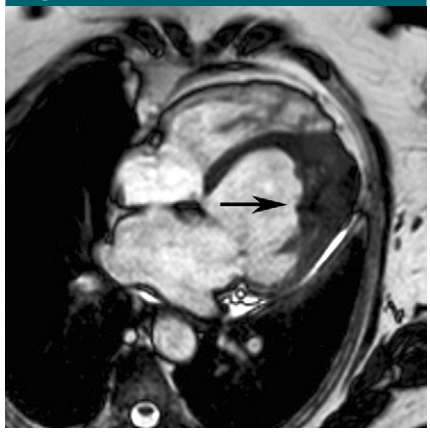

Figure 8: Endomyocardial disease in a 78-year-old woman with hypereosinophilia at presentation. Horizontal long-axis cine SSFP MR image (2.7/1.4, 55° flip angle, 1.4 × 2.0-mm in-plane resolution) demonstrates thickening and deformation of LV apex with cavity obliteration. The papillary muscles are involved in the inflammatory fibrotic process (arrow). (Image courtesy of Ilse Crevits, MD, Roeselare, Belgium.)

substantial decrease in T1 relaxation values and allowing differentiation with other diseases such as HCM, amyloidosis, and hypertensive disease (64).

Endomyocardial disease (ie, Löffler endocarditis and endomyocardial disease) is a rare form of restrictive cardiomyopathy that may simulate HCM. MR imaging enables depiction of the fibrous endocardial thickening, myocardial inflammation, apical or subvalvular obliteration, chordal deformation with valvular regurgitation, thrombus formation, and restrictive LV physiology (Fig 8). MR is particularly helpful in differentiating this entity from apical HCM and LV noncompaction (65). Finally, rare HCM phenocopies include primary and secondary cardiac tumors. In particular, cardiac fibromas and hemangiomas occur often intramurally and, when located in the anterior LV wall and ventricular septum, may simulate HCM. Cardiac metastases are more common than primary tumors and are usually found in patients with disseminated neoplasms. With use of comprehensive MR imaging, the differential diagnosis with HCM is usually straightforward.

Dynamic LV Outflow Tract Obstruction

Clinical Aspects

LV outflow tract obstruction is such a visible component of HCM that the disease has long been termed "hypertrophic obstructive cardiomyopathy (or HOCM)," assuming that all patients developed subaortic gradients related to systolic anterior motion and mitral septal contact (66). Large echocardiographic studies have later disproved this concept in patients at rest, most of whom appear to have nonobstructive disease. However, exercise echocardiography has recently reaffirmed the initial view, that is, that HCM is largely an obstructive disease, because of the high prevalence of provocable gradients on effort. A peak instantaneous outflow gradient of 30 mm Hg or greater under basal conditions or of 50 mm Hg or greater with exercise defines clinically significant dynamic obstruction, typically occurring during late systole and ranging from mild degrees of impedance to severe obstruction with gradients greater than 100 mm Hg. Besides the common subaortic obstruction, intraventricular gradients may be observed at the midventricular level and, rarely, at the right ventricular outflow tract.

Dynamic obstruction is a common cause of dyspnea, angina, and syncope on effort and is associated with increased risk of heart failure–related death (Table 2) (67). The pathophysiology of mitral leaflet systolic anterior motion is complex (38,39). During systole, abnormal acceleration and misdirection of the flow toward the outflow create "drag forces," which push the mitral leaflets anteriorly, causing septal contact and impedance to flow, as well as loss of coaptation and mitral regurgitation (Fig 9, Movie 3 [online]). The degree of mitral regurgitation may be moderate to severe, often with marked increase during exercise, ultimately promoting left atrial enlargement and atrial fibrillation. Because of a number of pathophysiologic determinants, outflow gradients may occur also in patients with minimal or no hypertrophy (66). Dynamic obstruction is initially managed medically, by using negative inotropes such as beta-blockers and/or disopyramide. However, when severe and associated with drug-refractory symptoms, invasive treatment options such as surgical myectomy or percutaneous alcohol ablation become necessary (68).

MR Imaging of LV Outflow Tract Obstruction

Echocardiography remains the technique of choice to rapidly, accurately, and serially evaluate the presence and hemodynamic impact of dynamic obstruction. However, MR imaging can provide valuable additional information regarding its site, mechanism, and potential management. For example, surgical planning may benefit from the superb anatomic detail of the mitral valve, subvalvar apparatus, and outflow tract offered by MR imaging. Longitudinal and perpendicular cine imaging through the LV outflow tract allows optimal visualization of systolic anterior motion and of the signal void caused by flow acceleration and/or turbulence at this level, as well as accurate measurement of diameter and/or area changes of the outflow tract over the cardiac cycle (Fig 9). An outflow tract of less than

2.7 cm^2 in systole measured by using MR imaging yielded a 100% sensitivity and specificity to differentiate obstructive (including latent forms) from nonobstructive HCM (69). In patients with severe midventricular and/or RV outflow tract obstruction, MR images provide critical anatomic details, instrumental to planning complex surgery. The combination of cine and velocity-encoded MR imaging allows direct measurement of outflow tract gradients and quantification of concomitant mitral regurgitation (Table 2, Fig 9) (52). However, to date, MR remains markedly inferior to Doppler echocardiography in the evaluation of flow velocity, particularly when assessment of gradients during exercise is required.

Microvascular Ischemia, Myocardial Fibrosis, and Disease Progression

Clinical Aspects

Autopsy findings in young patients with SCD have shown the presence of all stages of ischemic damage in HCM hearts, ranging from acute lesions to old replacement fibrosis (70). In the absence of epicardial coronary artery disease, ischemic damage is subtended by severe microvascular remodeling and dysfunction of the small intramural arterioles (Table 2) (71,72). Microvascular ischemia, which is most pronounced in—but not confined to—the hypertrophied regions, is important in the pathogenesis of disease progression and LV dysfunction and is a likely substrate for ventricular arrhythmias (22,73,74). Of note, microvascular dysfunction is more pronounced in gene-positive HCM patients compared with those without gene mutations (75), suggesting a molecular link between sarcomere mutations and microvascular remodeling (76).

The magnitude of replacement fibrosis is variable and correlates with severity of LV remodeling and dysfunction (76–78). Discrete areas of what is supposed to be replacement fibrosis are often seen in the midwall (mesocardium) of the most hypertrophied segments. In the most severe cases, transmural fibrotic tissue may occupy large portions of the LV wall, giving rise to pseudo-infarct patterns and the extreme degree of remodeling observed in end-stage HCM (Table 1) (Fig 10) (Movie 4 [online]) (28,29,79). In addition, extensive and transmural fibrosis consistently occurs in the walls of apical aneurysms associated with HCM. Replacement fibrosis represents a different phenomenon from the increased extracellular matrix commonly seen at the junction of the right ventricle with the LV—likely due to a different, nonischemic mechanism—and from the fine interstitial fibrosis that is diffusely found in HCM hearts. The stimulus for interstitial fibrosis, reflecting exaggerated activation of the matrix, may be present before the development of cardiac hypertrophy in genotype-positive individuals (80).

Figure 9

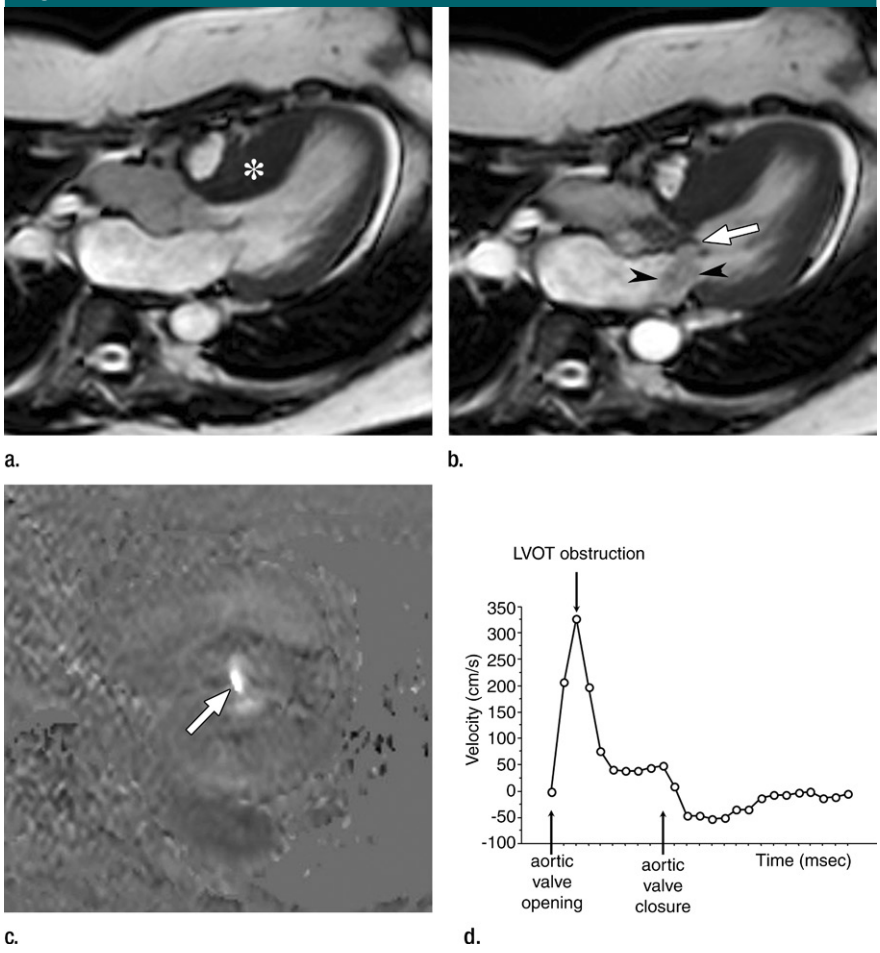

Figure 9: Obstructive HCM in a 57-year-old woman with heart failure and atrial fibrillation at presentation: **(a, b)** Cine SSFP MR images (2.7/1.4, 55° flip angle, 1.4 × 2.0-mm in-plane resolution) obtained longitudinally through LV outflow tract at **(a)** end diastole and **(b)** early systole depict thickened ventricular septum (25 mm) (*) with narrowing of LV outflow tract (11 mm), systolic anterior motion of anterior mitral valve leaflet (arrow, **b**) coming in apposition with thickened septum, and secondary mild regurgitation with laterally oriented jet (arrowheads, **b**). **(c)** Velocity-encoded cine MR image perpendicular through the LV outflow tract in early systole shows high velocity flow (peak velocity 3.5 m/sec) through the narrowed LV outflow tract (arrow). **(d)** The corresponding flow curve shows complete occlusion of LV outflow tract later in systole. This patient was treated by means of alcohol septal ablation. See Movie 3 (online).

Figure 10

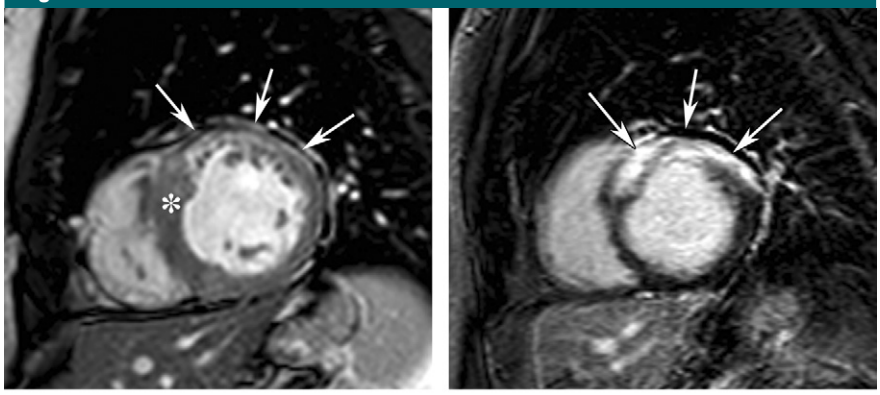

a. b.

Figure 10: Severe adverse remodeling in a 48-year-old man with HCM and history of SCD in multiple family members. **(a)** Short-axis cine SSFP MR image (2.7/1.4, 55° flip angle, 1.4 × 2.0-mm in-plane resolution) and **(b)** short-axis LGE MR image (4.3/1.3, inversion time 265 msec) show moderately dilated (end-diastolic volume, 190 mL) and dysfunctional LV (ejection fraction, 51%). Moderately thickened septum (15 mm) (*) and substantial thinning of the anterior LV wall (arrows, **a**) show marked enhancement (arrows, **b**). Total area of myocardial enhancement accounted for 23% of the whole LV mass. Note the dilated left atrium (21 cm^2/m^2) and pronounced myocardial trabeculations along the lateral LV wall and apex in Movie 4 (online). Electrophysiologic testing showed inducible polymorphic ventricular tachycardia and ventricular fibrillation. This patient received an implantable cardioverter defibrillator as primary prophylaxis of SCD.

Role of MR Imaging in Assessing Microvascular Dysfunction and Fibrosis

Though a great deal of our knowledge regarding microvascular ischemia in HCM should be credited to the use of SPECT and PET, MR imaging has now become an interesting alternative (21,81) because of its superior spatial resolution and its capability to help identify myocardial fibrosis (Table 3) (Fig 11) (Movie 5 [online]) (82–84). The perfusion MR sequences do not differ from those used in patients with coronary artery disease (eg, saturation-recovery fast gradient-echo sequence). Studies are typically performed at rest and during administration of a vasodilating agent (eg, dipyridamole). Areas of diminished myocardial perfusion can be visually assessed or semiquantitatively analyzed (as myocardial perfusion reserve ratio); absolute myocardial blood flow may also be calculated, but this procedure remains time consuming and largely confined to research purposes.

The introduction of LGE imaging, using two-dimensional or 3D inversion-recovery (or alternatively phase-sensitive inversion-recovery) gradient-echo sequences after administration of paramagnetic contrast agents, led to a paradigm shift in assessing ischemic and nonischemic myocardial disease (Figs 2, 5, 11) (85). Focal myocardial damage (eg, necrosis, replacement fibrosis) as small as 1 g or less is reliably depicted by LGE, while newer T1-mapping techniques appear promising in demonstrating interstitial fibrosis (86,87). To date, however, the optimal approach for defining and quantifying LGE in HCM remains unresolved (88). Image contrast following administration of gadolinium chelates is largely determined by the distribution volume (ie, the extracellular space) and washout characteristics of the contrast agent. However, contrary to the homogeneous, well-defined enhancement of scar tissue in patients with a healed myocardial infarction, the heterogeneous substrates present in HCM (ie, replacement fibrosis, interstitial fibrosis, and myofiber disarray) generate a spectrum of isolated or multiple patchy patterns of LGE (Figs 2, 5, 11) (89). Such complexity hampers any attempt toward reliable manual contouring and requires (semi)-automated analysis for quantification. By using signal intensity in normal (ie, nonthickened) myocardium as a reference, Harrigan et al (90) showed that use of 6 or more standard deviations from normal myocardial intensity had the best correlation with visual assessment. However, validation data from 29 myectomy specimens from HCM patients showed 5 standard deviations to have the strongest correlation with total (ie, combined interstitial and replacement) fibrosis, whereas the best correlation with replacement fibrosis was obtained at 10 standard deviations (91).

Since the first reports in 2002, LGE imaging has gained rapid interest as a potential tool to improve risk assessment in HCM patients, independent of conventional clinical predictors (4,92,93). A decade later, it is fair to say that several gaps remain in our knowledge (94). We have learned that LGE is a common finding occurring in the majority of HCM patients (range, 33%–79%) with highly variable extent and intensity (83,95) and, consistent with prior pathologic studies, preferentially localized to the midwall of regions with maximum LV wall thickness (Table 1) (70,96,97). Stress-perfusion defects are often found in the same regions expressing LGE, although typically located in the subendocardial region rather than at midwall (Fig 11). However, LGE may also be observed in HCM hearts with no evidence of microvascular ischemia (82–84).

In clinical practice, LGE imaging provides an excellent noninvasive tool to identify and monitor disease progression. Because the classic HCM phenotype is associated with preserved or increased LV ejection fraction and limited LGE (ie, <5%), adverse remodeling should be suspected when LV ejection fraction is below 65% and extent of LGE accounts for 10%–15% or more of the LV mass (Table 1) (29). These patients require close follow-up to serially evaluate the progression of fibrosis and its

Figure 11

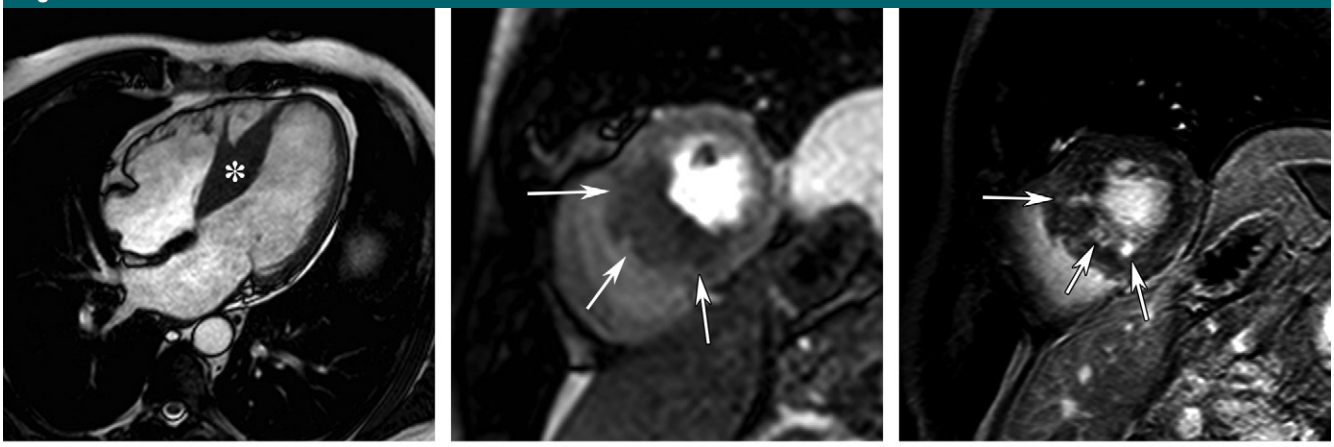

a. b. c.

Figure 11: Extensive microvascular dysfunction in 40-year-old man with asymmetric septal HCM. Images are **(a)** horizontal long-axis cine SSFP MR image (2.7/1.4, 55° flip angle, 1.4 × 2.0-mm in-plane resolution), **(b)** myocardial perfusion MR image during dipyridamole stress, and **(c)** LGE MR image in midventricular short axis. Thickening of the basal and midportions of the ventricular septum (*) is seen. A large perfusion defect is depicted in the thickened septum during dipyridamole stress (arrows, **b**) which is considerably more extensive than the patchy multifocal areas of late myocardial enhancement (arrows, **c**). See also Movie 5 (online).

Figure 12

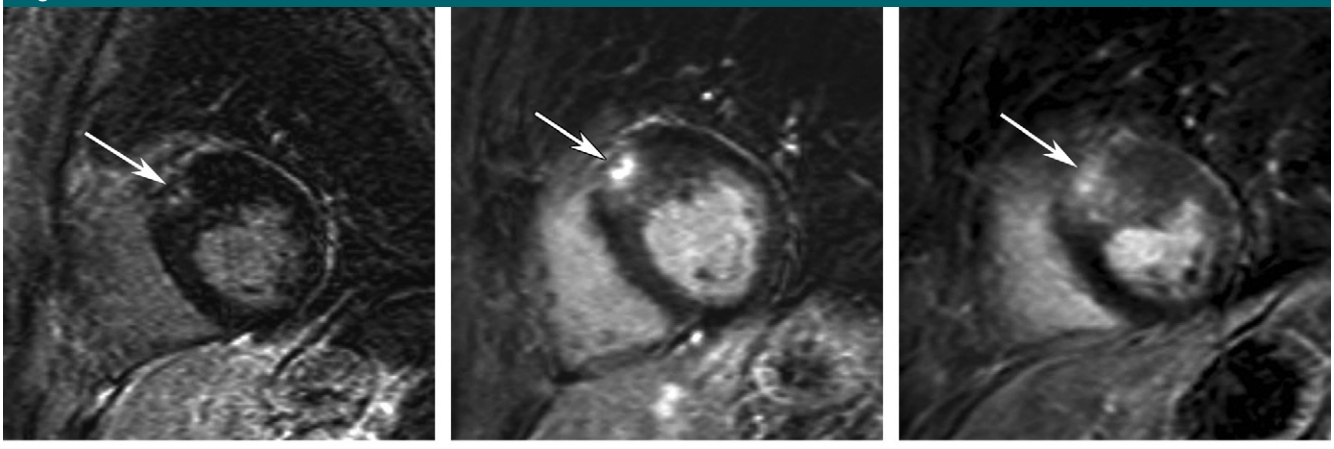

a. b. c.

Figure 12: Progression of myocardial enhancement, reflecting myocardial fibrosis over a period of 8 years in a 57-year-old woman with HCM: **(a)** baseline study, **(b)** first follow-up study at 5 years, and **(c)** second follow-up study at 8 years. On these short-axis LGE MR images (4.3/1.3, inversion time ranging between 250 and 290 msec), increase in size and intensity of myocardial enhancement can be seen in the anteroseptal LV wall (arrow).

functional consequences. Because of the considerable time elapsing from initial detection of LGE to overt LV impairment, identification of extensive remodeling may be relevant to preventive treatment (98).

In a recent study by Todiere et al (99), increases in myocardial LGE were shown in HCM patients during a mean follow-up period of nearly 2 years (Fig 12), predicting worsening clinical status. However, such widespread rapid increase in myocardial fibrosis is likely exaggerated by patient selection bias. In our experience, a similar time-course represents an exception rather than the rule in HCM patients, most of whom exhibit little or no change in LGE or clinical status in years. Overall, only 1%–2% of new patients per year will develop sufficiently severe remodeling to reach the end-stage phase of HCM, defined as a progressive systolic heart failure, often coupled with a restrictive LV filling pattern, heralding adverse outcome (100). Overt dysfunction is considered present when LV ejection fraction is below 50%—representing marked systolic impairment in this

Table 5

Risk Factors for SCD

Category	Factors
Secondary prevention	Cardiac arrest or sustained ventricular tachycardia
Conventional primary prevention risk predictors	Family history of SCD due to HCM
	Unexplained recent syncope
	Multiple, repetitive nonsustained ventricular tachycardia (on Holter)
	Abnormal blood pressure response to exercise
	Massive LV hypertrophy (thickness ≥ 30 mm)
	Extensive and diffuse LGE
Potential high-risk subsets for primary prevention	End-stage phase (LV ejection fraction < 50%)
	LV apical aneurysm and scarring
Potential arbitrators for primary prevention	Very early onset (pediatric age)
	Severe LV outflow tract gradient at rest
	Prior alcohol septal ablation
	Multiple sarcomere mutations
	Modifiable: intense competitive sports; coronary artery disease; atrial fibrillation with rapid ventricular conduction

Note.—Adapted, with permission, from reference 4.

Figure 13

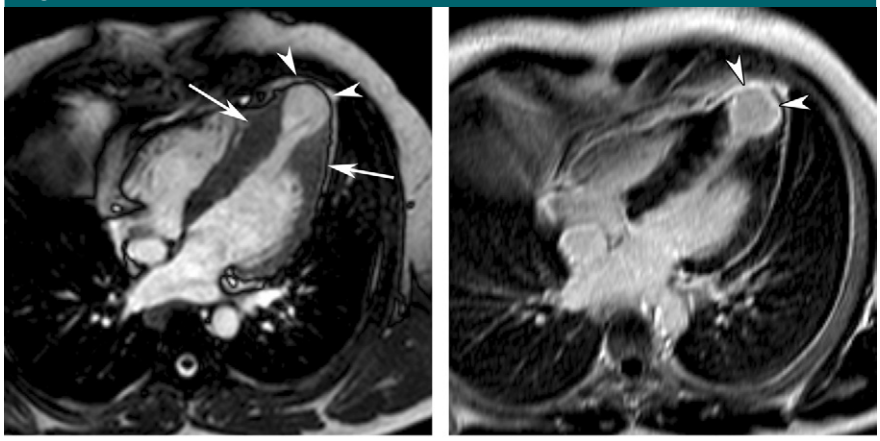

a. b.

Figure 13: Midventricular HCM with apical aneurysm in 40-year-old man. **(a)** Horizontal long-axis cine SSFP MR image (2.7/1.4, 55° flip angle, 1.4 × 2.0-mm in-plane resolution) and **(b)** LGE MR image (4.3/1.3, inversion time 265 msec) are shown. Note thickening of the midventricular part of the LV (arrows, **a**) with narrowing of LV cavity, apical wall thinning, and aneurysm formation (arrowheads, **a**). Transmural enhancement of the thinned apical wall (arrowheads, **b**) is seen. (Image courtesy of E. Algheri, MD, Department of Cardiovascular Imaging, Prof. Dr. Rémy-Jardin, University Center of Lille, Lille, France.)

disease, and is typically associated with extensive LGE (25%–50% of the whole LV) (101). Furthermore, predominance of midwall enhancement is lost, and extensive, often transmural enhancement predominates, associated with severe microvascular dysfunction, LV wall thinning, and loss of dynamic obstruction (Fig 10, Movie 4 [online]) (102). Of note, about half of the patients with end-stage HCM have a small and fibrosed, rather than dilated, LV associated with extreme diastolic dysfunction and biatrial dilatation, resembling restrictive cardiomyopathy (Table 1).

Sudden Cardiac Death

Clinical Aspects

SCD due to unpredictable ventricular tachyarrhythmias and ventricular fibrillation is the most visible and devastating complication of HCM, often occurring in asymptomatic individuals younger than 35 years and in competitive athletes (4). Fortunately, it is a rare occurrence, with a mean annual rate less than 1% (5). The identification of high-risk patients has become progressively more relevant to clinical practice following large-scale introduction of the implantable cardioverter defibrillator and is today one of the most hotly debated issues in HCM. Over the past 50 years, several SCD risk factors and potential risk modifiers have been identified from observational studies, allowing the construction of algorithms for risk stratification (Table 5). With the exception of a previous history of resuscitated cardiac arrest, however, these risk factors have very low positive predictive values (< 20%) (5). As a consequence, primary prevention of SCD remains challenging, and therapeutic strategies are often based on personal experience and individual preferences rather than solid evidence.

Potentially lethal ventricular arrhythmia in HCM originates from the interplay of multiple substrates and triggers ranging from microvascular ischemia to electrophysiologic remodeling of the cardiomyocyte (Table 2). Myofiber disarray, replacement, and interstitial myocardial fibrosis all may bear arrhythmogenic potential (4,29). This concept is supported by the observation that clinical examples of advanced fibrotic remodeling of the LV, such as apical aneurysms and end-stage HCM, both identify subsets with markedly increased risk of SCD, warranting aggressive management (Fig 13) (101,103).

Role of MR Imaging

Recently, LGE imaging has been recognized as a potential arbitrator in assessing risk of SCD (104). Several reports are consistent in highlighting the association of marked degrees of LGE with risk of arrhythmic events. However,

these studies were generally based on surrogate end points (such as nonsustained ventricular tachycardia) and underpowered to address SCD as an end point (96,97,105–107). Furthermore, as highlighted by Ismael et al (108), the key question is not only whether LGE is associated with arrhythmic events, but whether it adds independent prognostic value over and above traditional risk factors already in use.

Because LGE is common, its mere presence or absence is unlikely to have any clinical utility, so that the issue rather becomes whether its amount and extension may be predictive of outcome in individual patients. A recent multicenter, prospective study in 1300 consecutive HCM patients followed for more than 3 years has shown that extensive LGE, occupying 15% or more of whole LV myocardium, is an independent predictor of SCD (109), potentially relevant to decision making concerning cardioverter defibrillator implantation (Table 5). Of note, the same magnitude of LGE predicted heart failure–related events.

Atrial Fibrillation and Cardioembolic Risk

Clinical Aspects

Atrial fibrillation is the most common complication of HCM, occurring in nearly one-fourth of the patients, with an annual incidence of 2% (110). Predisposing factors include elevated LV end-diastolic pressures secondary to diastolic dysfunction, mitral regurgitation due to systolic anterior motion, and a primary myopathic process involving the atria (Table 2). Marked left atrial remodeling (ie, a combination of dilatation and fibrosis) generally constitutes the substrate for atrial fibrillation (111). True to its definition of "barometer" of the LV, left atrial size is an important predictor of outcome in HCM, independent of atrial fibrillation itself. In one study, an echocardiographic left atrial diameter larger than 48 mm (ie, the 75th percentile for the whole study group) predicted all-cause mortality, cardiovascular death, and death related to heart failure in HCM patients (112). The acute onset of atrial fibrillation, often occurring in young HCM patients, may be life-threatening when rapidly conducted to the LV resulting in hemodynamic destabilization. Long term, HCM patients with atrial fibrillation are at increased risk of stroke, peripheral embolization, heart failure complications, and death. Atrial fibrillation occurring in the context of LV outflow tract obstruction is poorly tolerated by HCM patients.

Role of MR Imaging in Atrial Fibrillation and Cardioembolic Risk Stratification

Volumetric determination by means of MR imaging is probably the best approach to assess the degree of atrial remodeling, but acquisition and analysis may be too time-consuming for daily clinical practice. Therefore, one- and two-dimensional measurements are a valuable alternative, with an area greater than 15 cm^2/m^2 and a transverse diameter greater than 2.8 cm/m^2 in four-chamber view generally used to identify left atrial enlargement (Movie 4 [online]) (113). In patients referred for catheter ablation of atrial fibrillation, a multiparametric MR imaging approach combining cine imaging with contrast-enhanced MR angiography and imaging early following contrast agent administration represents a valuable alternative to transesophageal echocardiography for evaluation of pulmonary vein anatomy and exclusion of thrombus in the left atrial appendage (Table 3) (114). Furthermore, LGE imaging enables the assessment of additional arrhythmic substrates and postablation lesions within the left atrium (115). Recently, ablation procedures in an MR environment have become feasible in the research setting, potentially opening the door for radiation-free procedures in HCM patients (116,117).

Planning and Assessing Clinical Interventions

Clinical Aspects

In HCM patients with severe drug-refractory symptoms of heart failure in the context of dynamic outflow obstruction, invasive septal reduction therapies are indicated. MR is becoming the tool of choice for preprocedural planning and assessment of local and remote remodeling during follow-up. Surgical septal myectomy represents the primary treatment option in these patients, whereas catheter-based techniques such as septal alcohol ablation and coil placement or, recently, the mitral clip, should be reserved to older patients at unacceptable surgical risk (5,118,119). Surgical treatment is a low-risk procedure that reliably abolishes impedance to LV outflow and heart failure symptoms, restores quality of life, and is associated with long-term survival similar to that of the general population (118,119). Moreover, myectomy can be tailored to the individual patient by combining reconstructive surgery of the papillary muscles and mitral valve chordae, as well as relief of midventricular and right ventricular outflow tract obstruction (120). Alcohol septal ablation creates a transmural scar at the basal septal level, thus enlarging LV outflow tract dimensions and relieving obstruction. New atrioventricular conduction abnormalities are frequent after septal ablation and are related to more extensive septal infarctions. Furthermore, the procedure is limited by the anatomic variability of the coronary tree, relief of obstruction is less consistent, and the iatrogenic scar has been associated with increased risk for life-threatening ventricular tachyarrhythmias (118,119).

Role of MR Imaging in Assessing Treatment

Multiparametric MR imaging provides an excellent tool to assess the effects of interventional treatment in HCM patients. A combination of cine, velocity-encoded, and LGE imaging provides comprehensive information on the LV anatomy, changes in postoperative morphology (including long-term reverse remodeling), myocardial substrate (location and extent of alcohol-induced scar), hemodynamic consequences, and procedure-related complications (121–125). Following alcohol septal ablation, a transmural

scar is typically produced in the basal septum, which tapers to nontransmural moving toward the mid-LV and usually extends into the right ventricular side of the septum (126). Moreover, in up to 25% of patients, the most proximal basal septum is spared, because of the lack of a septal branch supplying that region, accounting for suboptimal procedural results. The Amsterdam group studied the early and midterm effects of septal ablation in HCM patients (123–125). They observed that the induced infarct size correlated with gradient reduction and that, following relief of obstruction, an overall reduction in myocardial mass and improvement in systolic function occurred even in remote regions of the LV, suggesting regression of secondary hypertrophy. In the near future, MR-based studies will hopefully provide insights regarding the effects of pharmacologic treatments aimed at preventing development of LV hypertrophy and fibrosis. The identification of novel, disease-specific therapeutic targets, currently under investigation, may soon lead to the development of pharmacologic agents affecting some of the fundamental mechanisms of HCM pathogenesis (29). Trial design will necessarily incorporate serial MR evaluation in assessing the efficacy of these drugs.

Evaluation of Genotype-Positive/Phenotype-Negative Individuals

All mutation carriers are at risk for developing overt HCM. However, not all of them will, and whether (or to what extent) hypertrophy will develop remains unpredictable based on the individual genetic defect. Moreover, routine screening techniques such as echocardiography may fail to show mild abnormalities that precede a classic HCM phenotype. In one study, as many as 10% of mutation carriers with normal echocardiogram had some degree of LV hypertrophy at MR imaging (127). Furthermore, MR has shown great promise in the identification of genotype-positive individuals with phenotypic manifestations other than LV hypertrophy —a transition between pure mutation carrier status and overt HCM (Table 1) (29). For example, genotype-positive individuals may exhibit increased mitral leaflet dimensions (38), a trait similar to that seen in overt HCM. Furthermore, deep myocardial crypts are found in up to 81% of genotype-positive individuals without LV hypertrophy (Fig 14; Movie 6 [online]), compared with 6% in healthy volunteers (42,43). Notably, the identification of myocardial crypts is enhanced by use of additional nonconventional imaging planes, such as an additional stack of horizontal long-axis cine images through the inferior part of the LV (128). Another, recently described morphologic marker for HCM is the presence of an accessory apical-basal muscle bundle in the LV cavity, present in 63% of probands, in 60% of genotype-positive/phenotype-negative family members, but in only 10% of controls (129).

Recently, Ho et al (87), using T1-mapping, found increased myocardial extracellular volume in mutation carriers without LV hypertrophy, supporting the view that fibrotic remodeling is an early feature in the pathogenesis of the disease. T1 measurements correlated well with markers of collagen synthesis, suggesting that this technique may help monitor disease progression as well as to evaluate novel disease modifying therapy, targeting interstitial fibrosis.

Conclusion

After more than 50 years of extensive research, our understanding of the clinical spectrum of HCM has grown to an extent that would have been hardly predictable at the beginning of this journey. As the formidable complexity of HCM pathophysiology is being unraveled, new tools become necessary to address the central issues ultimately relevant for prevention and treatment. Few options like MR offer the opportunity of investigating the diverse morphologic, functional, and metabolic aspects of HCM hearts in vivo, opening novel avenues for the next half-century of investigation into this fascinating disease.

Disclosures of Conflicts of Interest: J.B. disclosed no relevant relationships. **I.O.** disclosed no relevant relationships.

Figure 14

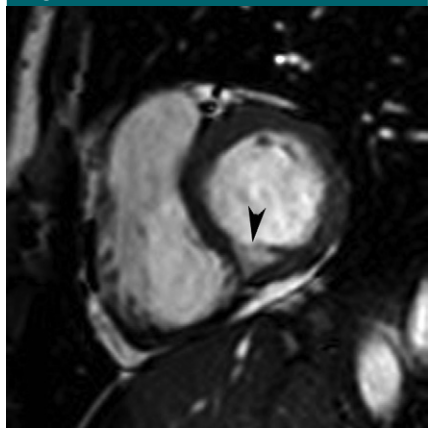

Figure 14: Presence of myocardial crypt in 25-year-old male mutation carrier (MYBPC3) with two prior episodes of syncope. Short-axis cine SSFP MR image (2.7/1.4, 55° flip angle, 1.4 × 2.0-mm in-plane resolution) shows borderline increase in LV wall thickness (13 mm) with presence of deep crypt in the inferoseptal LV wall (arrowhead). The myocardial crypt can be appreciated on Movie 6 (online).

References

1. Maron BJ, Towbin JA, Thiene G, et al. Contemporary definitions and classification of the cardiomyopathies: an American Heart Association Scientific Statement from the Council on Clinical Cardiology, Heart Failure and Transplantation Committee; Quality of Care and Outcomes Research and Functional Genomics and Translational Biology Interdisciplinary Working Groups; and Council on Epidemiology and Prevention. Circulation 2006;113(14):1807–1816.
2. Keren A, Syrris P, McKenna WJ. Hypertrophic cardiomyopathy: the genetic determinants of clinical disease expression. Nat Clin Pract Cardiovasc Med 2008;5(3):158–168.
3. Watkins H, Ashrafian H, Redwood C. Inherited cardiomyopathies. N Engl J Med 2011;364(17):1643–1656.
4. Maron BJ, Maron MS. Hypertrophic cardiomyopathy. Lancet 2013;381(9862):242–255.
5. Gersh BJ, Maron BJ, Bonow RO, et al. 2011 ACCF/AHA guideline for the diagnosis and treatment of hypertrophic cardiomyopathy: executive summary— a report of the American College of Cardiology Foundation/American Heart Association Task Force on Practice Guidelines. Circulation 2011;124(24):2761–2796.
6. Coats CJ, Hollman A. Hypertrophic cardiomyopathy: lessons from history. Heart 2008;94(10):1258–1263.

7. Brock R. Functional obstruction of the left ventricle: acquired aortic subvalvar stenosis. Guys Hosp Rep 1957;106(4):221–238.

8. Morrow AG, Braunwald E. Functional aortic stenosis: a malformation characterized by resistance to left ventricular outflow without anatomic obstruction. Circulation 1959;20(2):181–189.

9. Braunwald E, Lambrew CT, Rockoff SD, Ross J Jr, Morrow AG. Idiopathic hypertrophic subaortic stenosis. I. A description of the disease based upon an analysis of 64 patients. Circulation 1964;30(Suppl 4):3–119.

10. Teare D. Asymmetrical hypertrophy of the heart in young adults. Br Heart J 1958; 20(1):1–8.

11. Hollman A, Goodwin JF, Teare D, Renwick JW. A family with obstructive cardiomyopathy (asymmetrical hypertrophy). Br Heart J 1960;22:449–456.

12. Shah PM, Gramiak R, Kramer DH. Ultrasound localization of left ventricular outflow obstruction in hypertrophic obstructive cardiomyopathy. Circulation 1969;40(1):3–11.

13. Henry WL, Clark CE, Glancy DL, Epstein SE. Echocardiographic measurement of the left ventricular outflow gradient in idiopathic hypertrophic subaortic stenosis. N Engl J Med 1973;288(19):989–993.

14. Morrow AG, Fogarty TJ, Hannah H 3rd, Braunwald E. Operative treatment in idiopathic hypertrophic subaortic stenosis: techniques, and the results of preoperative and postoperative clinical and hemodynamic assessments. Circulation 1968;37(4):589–596.

15. Klues HG, Leuner C, Kuhn H. Left ventricular outflow tract obstruction in patients with hypertrophic cardiomyopathy: increase in gradient after exercise. J Am Coll Cardiol 1992;19(3):527–533.

16. Maron MS, Olivotto I, Zenovich AG, et al. Hypertrophic cardiomyopathy is predominantly a disease of left ventricular outflow tract obstruction. Circulation 2006; 114(21):2232–2239.

17. Klues HG, Roberts WC, Maron BJ. Anomalous insertion of papillary muscle directly into anterior mitral leaflet in hypertrophic cardiomyopathy: significance in producing left ventricular outflow obstruction. Circulation 1991;84(3):1188–1197.

18. Klues HG, Roberts WC, Maron BJ. Morphological determinants of echocardiographic patterns of mitral valve systolic anterior motion in obstructive hypertrophic cardiomyopathy. Circulation 1993;87(5):1570–1579.

19. Clark CE, Henry WL, Epstein SE. Familial prevalence and genetic transmission of idiopathic hypertrophic subaortic stenosis. N Engl J Med 1973;289(14):709–714.

20. O'Gara PT, Bonow RO, Maron BJ, et al. Myocardial perfusion abnormalities in patients with hypertrophic cardiomyopathy: assessment with thallium-201 emission computed tomography. Circulation 1987; 76(6):1214–1223.

21. Nienaber CA, Gambhir SS, Mody FV, et al. Regional myocardial blood flow and glucose utilization in symptomatic patients with hypertrophic cardiomyopathy. Circulation 1993;87(5):1580–1590.

22. Cecchi F, Olivotto I, Gistri R, Lorenzoni R, Chiriatti G, Camici PG. Coronary microvascular dysfunction and prognosis in hypertrophic cardiomyopathy. N Engl J Med 2003; 349(11):1027–1035.

23. Chun EJ, Choi SI, Jin KN, et al. Hypertrophic cardiomyopathy: assessment with MR imaging and multidetector CT. RadioGraphics 2010;30(5):1309–1328.

24. Basso C, Thiene G, Mackey-Bojack S, Frigo AC, Corrado D, Maron BJ. Myocardial bridging, a frequent component of the hypertrophic cardiomyopathy phenotype, lacks systematic association with sudden cardiac death. Eur Heart J 2009;30(13):1627–1634.

25. Nagueh SF, Bierig SM, Budoff MJ, et al. American Society of Echocardiography clinical recommendations for multimodality cardiovascular imaging of patients with hypertrophic cardiomyopathy: Endorsed by the American Society of Nuclear Cardiology, Society for Cardiovascular Magnetic Resonance, and Society of Cardiovascular Computed Tomography. J Am Soc Echocardiogr 2011;24(5):473–498.

26. Maron BJ, Spirito P, Wesley Y, Arce J. Development and progression of left ventricular hypertrophy in children with hypertrophic cardiomyopathy. N Engl J Med 1986;315(10):610–614.

27. Thaman R, Gimeno JR, Reith S, et al. Progressive left ventricular remodeling in patients with hypertrophic cardiomyopathy and severe left ventricular hypertrophy. J Am Coll Cardiol 2004;44(2):398–405.

28. Harris KM, Spirito P, Maron MS, et al. Prevalence, clinical profile, and significance of left ventricular remodeling in the end-stage phase of hypertrophic cardiomyopathy. Circulation 2006;114(3):216–225.

29. Olivotto I, Cecchi F, Poggesi C, Yacoub MH. Patterns of disease progression in hypertrophic cardiomyopathy: an individualized approach to clinical staging. Circ Heart Fail 2012;5(4):535–546.

30. Klues HG, Schiffers A, Maron BJ. Phenotypic spectrum and patterns of left ventricular hypertrophy in hypertrophic cardiomyopathy: morphologic observations and significance as assessed by two-dimensional echocardiography in 600 patients. J Am Coll Cardiol 1995;26(7):1699–1708.

31. Olivotto I, Maron MS, Autore C, et al. Assessment and significance of left ventricular mass by cardiovascular magnetic resonance in hypertrophic cardiomyopathy. J Am Coll Cardiol 2008;52(7):559–566.

32. Maron MS, Maron BJ, Harrigan C, et al. Hypertrophic cardiomyopathy phenotype revisited after 50 years with cardiovascular magnetic resonance. J Am Coll Cardiol 2009;54(3):220–228.

33. Maron MS, Hauser TH, Dubrow E, et al. Right ventricular involvement in hypertrophic cardiomyopathy. Am J Cardiol 2007;100(8):1293–1298.

34. Florian A, Masci PG, De Buck S, et al. Geometric assessment of asymmetric septal hypertrophic cardiomyopathy by CMR. JACC Cardiovasc Imaging 2012;5(7):702–711.

35. Moon JC, Fisher NG, McKenna WJ, Pennell DJ. Detection of apical hypertrophic cardiomyopathy by cardiovascular magnetic resonance in patients with non-diagnostic echocardiography. Heart 2004;90(6):645–649.

36. Bogaert J, Rademakers FE. Regional nonuniformity of normal adult human left ventricle. Am J Physiol Heart Circ Physiol 2001;280(2):H610–H620.

37. Maron MS, Finley JJ, Bos JM, et al. Prevalence, clinical significance, and natural history of left ventricular apical aneurysms in hypertrophic cardiomyopathy. Circulation 2008;118(15):1541–1549.

38. Maron MS, Olivotto I, Harrigan C, et al. Mitral valve abnormalities identified by cardiovascular magnetic resonance represent a primary phenotypic expression of hypertrophic cardiomyopathy. Circulation 2011;124(1):40–47.

39. Harrigan CJ, Appelbaum E, Maron BJ, et al. Significance of papillary muscle abnormalities identified by cardiovascular magnetic resonance in hypertrophic cardiomyopathy. Am J Cardiol 2008;101(5):668–673.

40. Kwon DH, Setser RM, Thamilarasan M, et al. Abnormal papillary muscle morphology is independently associated with increased left ventricular outflow tract obstruction in hypertrophic cardiomyopathy. Heart 2008; 94(10):1295–1301.

41. Germans T, Wilde AA, Dijkmans PA, et al. Structural abnormalities of the inferoseptal left ventricular wall detected by cardiac

magnetic resonance imaging in carriers of hypertrophic cardiomyopathy mutations. J Am Coll Cardiol 2006;48(12):2518–2523.

42. Maron MS, Rowin EJ, Lin D, et al. Prevalence and clinical profile of myocardial crypts in hypertrophic cardiomyopathy. Circ Cardiovasc Imaging 2012;5(4):441–447.

43. Brouwer WP, Germans T, Head MC, et al. Multiple myocardial crypts on modified long-axis view are a specific finding in pre-hypertrophic HCM mutation carriers. Eur Heart J Cardiovasc Imaging 2012;13(4):292–297.

44. Yetman AT, McCrindle BW, MacDonald C, Freedom RM, Gow R. Myocardial bridging in children with hypertrophic cardiomyopathy: a risk factor for sudden death. N Engl J Med 1998;339(17):1201–1209.

45. Maron MS. Clinical utility of cardiovascular magnetic resonance in hypertrophic cardiomyopathy. J Cardiovasc Magn Reson 2012;14:13.

46. To AC, Dhillon A, Desai MY. Cardiac magnetic resonance in hypertrophic cardiomyopathy. JACC Cardiovasc Imaging 2011;4(10):1123–1137.

47. Rickers C, Wilke NM, Jerosch-Herold M, et al. Utility of cardiac magnetic resonance imaging in the diagnosis of hypertrophic cardiomyopathy. Circulation 2005;112(6):855–861.

48. Scharhag J, Schneider G, Urhausen A, Rochette V, Kramann B, Kindermann W. Athlete's heart: right and left ventricular mass and function in male endurance athletes and untrained individuals determined by magnetic resonance imaging. J Am Coll Cardiol 2002;40(10):1856–1863.

49. Petersen SE, Selvanayagam JB, Francis JM, et al. Differentiation of athlete's heart from pathological forms of cardiac hypertrophy by means of geometric indices derived from cardiovascular magnetic resonance. J Cardiovasc Magn Reson 2005;7(3):551–558.

50. Maron BJ, Pelliccia A, Spirito P. Cardiac disease in young trained athletes: insights into methods for distinguishing athlete's heart from structural heart disease, with particular emphasis on hypertrophic cardiomyopathy. Circulation 1995;91(5):1596–1601.

51. Lauschke J, Maisch B. Athlete's heart or hypertrophic cardiomyopathy? Clin Res Cardiol 2009;98(2):80–88.

52. Masci PG, Dymarkowski S, Bogaert J. Valvular heart disease: what does cardiovascular MRI add? Eur Radiol 2008;18(2):197–208.

53. Ganau A, Devereux RB, Roman MJ, et al. Patterns of left ventricular hypertrophy and geometric remodeling in essential hypertension. J Am Coll Cardiol 1992;19(7):1550–1558.

54. Oechslin E, Jenni R. Left ventricular non-compaction revisited: a distinct phenotype with genetic heterogeneity? Eur Heart J 2011;32(12):1446–1456.

55. Gati S, Chandra N, Bennett RL, et al. Increased left ventricular trabeculation in highly trained athletes: do we need more stringent criteria for the diagnosis of left ventricular non-compaction in athletes? Heart 2013;99(6):401–408.

56. Petersen SE, Selvanayagam JB, Wiesmann F, et al. Left ventricular non-compaction: insights from cardiovascular magnetic resonance imaging. J Am Coll Cardiol 2005;46(1):101–105.

57. Jacquier A, Thuny F, Jop B, et al. Measurement of trabeculated left ventricular mass using cardiac magnetic resonance imaging in the diagnosis of left ventricular non-compaction. Eur Heart J 2010;31(9):1098–1104.

58. Falk RH, Dubrey SW. Amyloid heart disease. Prog Cardiovasc Dis 2010;52(4):347–361.

59. Banypersad SM, Sado DM, Flett AS, et al. Quantification of myocardial extracellular volume fraction in systemic AL amyloidosis: an equilibrium contrast cardiovascular magnetic resonance study. Circ Cardiovasc Imaging 2013;6(1):34–39.

60. Maceira AM, Joshi J, Prasad SK, et al. Cardiovascular magnetic resonance in cardiac amyloidosis. Circulation 2005;111(2):186–193.

61. Syed IS, Glockner JF, Feng D, et al. Role of cardiac magnetic resonance imaging in the detection of cardiac amyloidosis. JACC Cardiovasc Imaging 2010;3(2):155–164.

62. Karamitsos TD, Piechnik SK, Banypersad SM, et al. Noncontrast T1 mapping for the diagnosis of cardiac amyloidosis. JACC Cardiovasc Imaging 2013;6(4):488–497.

63. Moon JC, Sachdev B, Elkington AG, et al. Gadolinium enhanced cardiovascular magnetic resonance in Anderson-Fabry disease: evidence for a disease specific abnormality of the myocardial interstitium. Eur Heart J 2003;24(23):2151–2155.

64. Sado DM, White SK, Piechnik SK, et al. Identification and assessment of Anderson-Fabry disease by cardiovascular magnetic resonance noncontrast myocardial T1 mapping. Circ Cardiovasc Imaging 2013;6(3):392–398.

65. Pitt M, Davies MK, Brady AJ. Hypereosinophilic syndrome: endomyocardial fibrosis. Heart 1996;76(4):377–378.

66. Maron BJ, Maron MS, Wigle ED, Braunwald E. The 50-year history, controversy, and clinical implications of left ventricular outflow tract obstruction in hypertrophic cardiomyopathy from idiopathic hypertrophic subaortic stenosis to hypertrophic cardiomyopathy: from idiopathic hypertrophic subaortic stenosis to hypertrophic cardiomyopathy. J Am Coll Cardiol 2009;54(3):191–200.

67. Maron MS, Olivotto I, Betocchi S, et al. Effect of left ventricular outflow tract obstruction on clinical outcome in hypertrophic cardiomyopathy. N Engl J Med 2003;348(4):295–303.

68. Ommen SR, Maron BJ, Olivotto I, et al. Long-term effects of surgical septal myectomy on survival in patients with obstructive hypertrophic cardiomyopathy. J Am Coll Cardiol 2005;46(3):470–476.

69. Schulz-Menger J, Abdel-Aty H, Busjahn A, et al. Left ventricular outflow tract planimetry by cardiovascular magnetic resonance differentiates obstructive from non-obstructive hypertrophic cardiomyopathy. J Cardiovasc Magn Reson 2006;8(5):741–746.

70. Basso C, Thiene G, Corrado D, Buja G, Melacini P, Nava A. Hypertrophic cardiomyopathy and sudden death in the young: pathologic evidence of myocardial ischemia. Hum Pathol 2000;31(8):988–998.

71. Knaapen P, Germans T, Camici PG, et al. Determinants of coronary microvascular dysfunction in symptomatic hypertrophic cardiomyopathy. Am J Physiol Heart Circ Physiol 2008;294(2):H986–H993.

72. Kwon DH, Smedira NG, Rodriguez ER, et al. Cardiac magnetic resonance detection of myocardial scarring in hypertrophic cardiomyopathy: correlation with histopathology and prevalence of ventricular tachycardia. J Am Coll Cardiol 2009;54(3):242–249.

73. Varnava AM, Elliott PM, Sharma S, McKenna WJ, Davies MJ. Hypertrophic cardiomyopathy: the interrelation of disarray, fibrosis, and small vessel disease. Heart 2000;84(5):476–482.

74. Sotgia B, Sciagrà R, Olivotto I, et al. Spatial relationship between coronary microvascular dysfunction and delayed contrast enhancement in patients with hypertrophic cardiomyopathy. J Nucl Med 2008;49(7):1090–1096.

75. Olivotto I, Girolami F, Sciagrà R, et al. Microvascular function is selectively impaired in patients with hypertrophic cardiomyopathy and sarcomere myofilament gene mutations. J Am Coll Cardiol 2011;58(8):839–848.

76. Olivotto I, Cecchi F, Poggesi C, Yacoub MH. Developmental origins of hypertrophic car-

diomyopathy phenotypes: a unifying hypothesis. Nat Rev Cardiol 2009;6(4):317–321.

77. Bogaert J, Goldstein M, Tannouri F, Golzarian J, Dymarkowski S. Original report. Late myocardial enhancement in hypertrophic cardiomyopathy with contrast-enhanced MR imaging. AJR Am J Roentgenol 2003;180(4):981–985.

78. Esposito A, De Cobelli F, Perseghin G, et al. Impaired left ventricular energy metabolism in patients with hypertrophic cardiomyopathy is related to the extension of fibrosis at delayed gadolinium-enhanced magnetic resonance imaging. Heart 2009;95(3):228–233.

79. Melacini P, Basso C, Angelini A, et al. Clinicopathological profiles of progressive heart failure in hypertrophic cardiomyopathy. Eur Heart J 2010;31(17):2111–2123.

80. Ho CY, López B, Coelho-Filho OR, et al. Myocardial fibrosis as an early manifestation of hypertrophic cardiomyopathy. N Engl J Med 2010;363(6):552–563.

81. Olivotto I, Cecchi F, Gistri R, et al. Relevance of coronary microvascular flow impairment to long-term remodeling and systolic dysfunction in hypertrophic cardiomyopathy. J Am Coll Cardiol 2006;47(5):1043–1048.

82. Petersen SE, Jerosch-Herold M, Hudsmith LE, et al. Evidence for microvascular dysfunction in hypertrophic cardiomyopathy: new insights from multiparametric magnetic resonance imaging. Circulation 2007;115(18):2418–2425.

83. Tyan CC, Armstrong S, Scholl D, et al. Stress hypoperfusion and tissue injury in hypertrophic cardiomyopathy: spatial characterization using high-resolution 3-tesla magnetic resonance imaging. Circ Cardiovasc Imaging 2013;6(2):229–238.

84. Bravo PE, Zimmerman SL, Luo H-C, et al. Relationship of delayed enhancement by magnetic resonance to myocardial perfusion by positron emission tomography in hypertrophic cardiomyopathy. Circ Cardiovasc Imaging 2013;6(2):210–217.

85. Simonetti OP, Kim RJ, Fieno DS, et al. An improved MR imaging technique for the visualization of myocardial infarction. Radiology 2001;218(1):215–223.

86. Amano Y, Takayama M, Kumita S. Contrast-enhanced myocardial T1-weighted scout (Look-Locker) imaging for the detection of myocardial damages in hypertrophic cardiomyopathy. J Magn Reson Imaging 2009;30(4):778–784.

87. Ho CY, Abbasi SA, Neilan TG, et al. T1 measurements identify extracellular volume expansion in hypertrophic cardiomyopathy sarcomere mutation carriers with and without left ventricular hypertrophy. Circ Cardiovasc Imaging 2013;6(3):415–422.

88. Maron MS. Contrast-enhanced CMR in HCM: what lies behind the bright light of LGE and why it now matters. JACC Cardiovasc Imaging 2013;6(5):597–599.

89. Moon JC, Reed E, Sheppard MN, et al. The histologic basis of late gadolinium enhancement cardiovascular magnetic resonance in hypertrophic cardiomyopathy. J Am Coll Cardiol 2004;43(12):2260–2264.

90. Harrigan CJ, Peters DC, Gibson CM, et al. Hypertrophic cardiomyopathy: quantification of late gadolinium enhancement with contrast-enhanced cardiovascular MR imaging. Radiology 2011;258(1):128–133.

91. Moravsky G, Ofek E, Rakowski H, et al. Myocardial fibrosis in hypertrophic cardiomyopathy: accurate reflection of histopathological findings by CMR. JACC Cardiovasc Imaging 2013;6(5):587–596.

92. Choudhury L, Mahrholdt H, Wagner A, et al. Myocardial scarring in asymptomatic or mildly symptomatic patients with hypertrophic cardiomyopathy. J Am Coll Cardiol 2002;40(12):2156–2164.

93. Moon JC, McKenna WJ, McCrohon JA, Elliott PM, Smith GC, Pennell DJ. Toward clinical risk assessment in hypertrophic cardiomyopathy with gadolinium cardiovascular magnetic resonance. J Am Coll Cardiol 2003;41(9):1561–1567.

94. Appelbaum E, Maron BJ, Adabag S, et al. Intermediate-signal-intensity late gadolinium enhancement predicts ventricular tachyarrhythmias in patients with hypertrophic cardiomyopathy. Circ Cardiovasc Imaging 2012;5(1):78–85.

95. Noureldin RA, Liu S, Nacif MS, et al. The diagnosis of hypertrophic cardiomyopathy by cardiovascular magnetic resonance. J Cardiovasc Magn Reson 2012;14:17.

96. Rubinshtein R, Glockner JF, Ommen SR, et al. Characteristics and clinical significance of late gadolinium enhancement by contrast-enhanced magnetic resonance imaging in patients with hypertrophic cardiomyopathy. Circ Heart Fail 2010;3(1):51–58.

97. Bruder O, Wagner A, Jensen CJ, et al. Myocardial scar visualized by cardiovascular magnetic resonance imaging predicts major adverse events in patients with hypertrophic cardiomyopathy. J Am Coll Cardiol 2010;56(11):875–887.

98. Spoladore R, Maron MS, D'Amato R, Camici PG, Olivotto I. Pharmacological treatment options for hypertrophic cardiomyopathy: high time for evidence. Eur Heart J 2012;33(14):1724–1733.

99. Todiere G, Aquaro GD, Piaggi P, et al. Progression of myocardial fibrosis assessed with cardiac magnetic resonance in hypertrophic cardiomyopathy. J Am Coll Cardiol 2012;60(10):922–929.

100. Yacoub MH, Olivotto I, Cecchi F. 'End-stage' hypertrophic cardiomyopathy: from mystery to model. Nat Clin Pract Cardiovasc Med 2007;4(5):232–233.

101. Maron MS, Appelbaum E, Harrigan CJ, et al. Clinical profile and significance of delayed enhancement in hypertrophic cardiomyopathy. Circ Heart Fail 2008;1(3):184–191.

102. Thaman R, Gimeno JR, Reith S, et al. Progressive left ventricular remodeling in patients with hypertrophic cardiomyopathy and severe left ventricular hypertrophy. J Am Coll Cardiol 2004;44(2):398–405.

103. Minami Y, Kajimoto K, Terajima Y, et al. Clinical implications of midventricular obstruction in patients with hypertrophic cardiomyopathy. J Am Coll Cardiol 2011;57(23):2346–2355.

104. Green JJ, Berger JS, Kramer CM, Salerno M. Prognostic value of late gadolinium enhancement in clinical outcomes for hypertrophic cardiomyopathy. JACC Cardiovasc Imaging 2012;5(4):370–377.

105. Adabag AS, Maron BJ, Appelbaum E, et al. Occurrence and frequency of arrhythmias in hypertrophic cardiomyopathy in relation to delayed enhancement on cardiovascular magnetic resonance. J Am Coll Cardiol 2008;51(14):1369–1374.

106. Kwon DH, Setser RM, Popović ZB, et al. Association of myocardial fibrosis, electrocardiography and ventricular tachyarrhythmia in hypertrophic cardiomyopathy: a delayed contrast enhanced MRI study. Int J Cardiovasc Imaging 2008;24(6):617–625.

107. O'Hanlon R, Grasso A, Roughton M, et al. Prognostic significance of myocardial fibrosis in hypertrophic cardiomyopathy. J Am Coll Cardiol 2010;56(11):867–874.

108. Ismail TF, Prasad SK, Pennell DJ. Prognostic importance of late gadolinium enhancement cardiovascular magnetic resonance in cardiomyopathy. Heart 2012;98(6):438–442.

109. Chan RH, Maron B, Olivotto I, et al. Prognostic utility of contrast-enhanced cardiovascular magnetic resonance in hypertrophic cardiomyopathy: an international multicenter study. J Am Coll Cardiol 2012;59(13 Suppl):E1570.

110. Olivotto I, Cecchi F, Casey SA, Dolara A, Traverse JH, Maron BJ. Impact of atrial fibril-

lation on the clinical course of hypertrophic cardiomyopathy. Circulation 2001;104(21):2517–2524.

111. Darby AE, Dimarco JP. Management of atrial fibrillation in patients with structural heart disease. Circulation 2012;125(7):945–957.

112. Nistri S, Olivotto I, Betocchi S, et al. Prognostic significance of left atrial size in patients with hypertrophic cardiomyopathy (from the Italian Registry for Hypertrophic Cardiomyopathy). Am J Cardiol 2006;98(7):960–965.

113. Di Donna P, Olivotto I, Delcrè SD, et al. Efficacy of catheter ablation for atrial fibrillation in hypertrophic cardiomyopathy: impact of age, atrial remodelling, and disease progression. Europace 2010;12(3):347–355.

114. Maceira AM, Cosín-Sales J, Roughton M, Prasad SK, Pennell DJ. Reference left atrial dimensions and volumes by steady state free precession cardiovascular magnetic resonance. J Cardiovasc Magn Reson 2010;12:65.

115. Rathi VK, Reddy ST, Anreddy S, et al. Contrast-enhanced CMR is equally effective as TEE in the evaluation of left atrial appendage thrombus in patients with atrial fibrillation undergoing pulmonary vein isolation procedure. Heart Rhythm 2013;10(7):1021–1027.

116. Vergara GR, Marrouche NF. Tailored management of atrial fibrillation using a LGE-MRI based model: from the clinic to the electrophysiology laboratory. J Cardiovasc Electrophysiol 2011;22(4):481–487.

117. Ganesan AN, Selvanayagam JB, Mahajan R, et al. Mapping and ablation of the pulmonary veins and cavo-tricuspid isthmus with a magnetic resonance imaging-compatible externally irrigated ablation catheter and integrated electrophysiology system. Circ Arrhythm Electrophysiol 2012;5(6):1136–1142.

118. Maron BJ, Yacoub M, Dearani JA. Controversies in cardiovascular medicine. Benefits of surgery in obstructive hypertrophic cardiomyopathy: bring septal myectomy back for European patients. Eur Heart J 2011;32(9):1055–1058.

119. Iacovoni A, Spirito P, Simon C, et al. A contemporary European experience with surgical septal myectomy in hypertrophic cardiomyopathy. Eur Heart J 2012;33(16):2080–2087.

120. Schoendube FA, Klues HG, Reith S, Flachskampf FA, Hanrath P, Messmer BJ. Long-term clinical and echocardiographic follow-up after surgical correction of hypertrophic obstructive cardiomyopathy with extended myectomy and reconstruction of the subvalvular mitral apparatus. Circulation 1995;92(9 Suppl):II122–II127.

121. Olivotto I, Ommen SR, Maron MS, Cecchi F, Maron BJ. Surgical myectomy versus alcohol septal ablation for obstructive hypertrophic cardiomyopathy: will there ever be a randomized trial? J Am Coll Cardiol 2007;50(9):831–834.

122. Schulz-Menger J, Strohm O, Waigand J, Uhlich F, Dietz R, Friedrich MG. The value of magnetic resonance imaging of the left ventricular outflow tract in patients with hypertrophic obstructive cardiomyopathy after septal artery embolization. Circulation 2000;101(15):1764–1766.

123. van Dockum WG, ten Cate FJ, ten Berg JM, et al. Myocardial infarction after percutaneous transluminal septal myocardial ablation in hypertrophic obstructive cardiomyopathy: evaluation by contrast-enhanced magnetic resonance imaging. J Am Coll Cardiol 2004;43(1):27–34.

124. van Dockum WG, Beek AM, ten Cate FJ, et al. Early onset and progression of left ventricular remodeling after alcohol septal ablation in hypertrophic obstructive cardiomyopathy. Circulation 2005;111(19):2503–2508.

125. McCann GP, Van Dockum WG, Beek AM, et al. Extent of myocardial infarction and reverse remodeling assessed by cardiac magnetic resonance in patients with and without right bundle branch block following alcohol septal ablation for obstructive hypertrophic cardiomyopathy. Am J Cardiol 2007;99(4):563–567.

126. Valeti US, Nishimura RA, Holmes DR, et al. Comparison of surgical septal myectomy and alcohol septal ablation with cardiac magnetic resonance imaging in patients with hypertrophic obstructive cardiomyopathy. J Am Coll Cardiol 2007;49(3):350–357.

127. Valente AM, Lakdawala NK, Powell AJ, et al. Comparison of echocardiographic and cardiac magnetic resonance imaging in hypertrophic cardiomyopathy sarcomere mutation carriers without left ventricular hypertrophy. Circ Cardiovasc Genet 2013;6(3):230–237.

128. Deva DP, Williams LK, Care M, et al. Deep basal inferoseptal crypts occur more commonly in patients with hypertrophic cardiomyopathy due to disease-causing myofilament mutations. Radiology 2013;269(1):68–76.

129. Gruner C, Chan RH, Crean A, et al. Significance of left ventricular apical-basal muscle bundle identified by cardiovascular magnetic resonance imaging in patients with hypertrophic cardiomyopathy. Eur Heart J 2014 May 8. [Epub ahead of print]